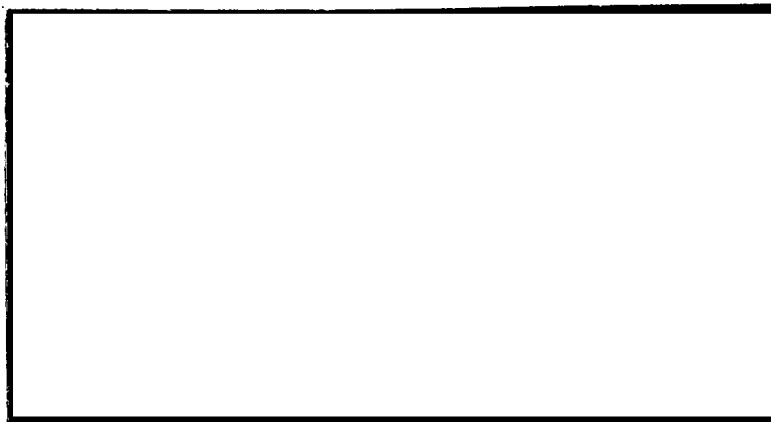


11
m/17



D.R.S

(NASA-CR-128172) AN INVARIANT SECOND-ORDER
 CLOSURE MODEL OF THE COMPRESSIBLE TURBULENT
 BOUNDARY LAYER ON A FLAT C.D. Donaldson,
 et al (Aeronautical Research Associates of
 Princeton) Jun. 1972 47 p CSCL 20D G3/01 16224
 N72-31993
 Unclass

A. R. A. P.

AERONAUTICAL RESEARCH ASSOCIATES of PRINCETON, INC.

Reproduced by
**NATIONAL TECHNICAL
 INFORMATION SERVICE**
 U S Department of Commerce
 Springfield VA 22151

FINAL REPORT

AN INVARIANT SECOND-ORDER
CLOSURE MODEL
OF THE COMPRESSIBLE
TURBULENT BOUNDARY LAYER
ON A FLAT PLATE

by

Coleman duP. Donaldson

and

Roger D. Sullivan

Prepared for

NASA Headquarters
Headquarters Contracts Division
Washington, D. C. 20546

under Contract No. NASW-2224

June 1972

I

N O T I C E

THIS DOCUMENT HAS BEEN REPRODUCED FROM THE BEST COPY FURNISHED US BY THE SPONSORING AGENCY. ALTHOUGH IT IS RECOGNIZED THAT CERTAIN PORTIONS ARE ILLEGIBLE, IT IS BEING RELEASED IN THE INTEREST OF MAKING AVAILABLE AS MUCH INFORMATION AS POSSIBLE.

NOMENCLATURE

Some symbols which are used only in small parts of the paper are defined there but omitted from this table.

General tensor notation is used in the first part of the analysis. In particular, the summation convention is implied, and a comma preceding a subscript indicates covariant differentiation.

c_f	- local skin friction coefficient
c_p	- specific heat at constant pressure
c_v	- specific heat at constant volume
e	- internal energy
g_{ij}	- matrix tensor
G_w	- ratio of wall temperature to free stream stagnation temperature, T_w/T_e^0
H	- see Eq. (7)
k	- <u>conductivity</u>
K	- $u^i \ell u^i_\ell$
M	- Mach number
p	- pressure
p_T	- dimensionless constant
q	- \sqrt{K}
R	- gas constant
Re_x	- Reynolds number based on distance from the leading edge, $\rho_e u_e x / \mu_e$
St	- Stanton number, $\frac{(k \partial T / \partial y)_w}{c_p \rho_e u_e (T_{aw} - T_w)}$
T	- absolute temperature

T_{aw}	- adiabatic wall temperature
T_e^0	- free stream stagnation temperature
u_i or u, v, w ,	- velocity components
V_c, V_{VT}, V_{TT}	- dimensionless constants
x_i or x, y, z	- coordinate system
δ_j^i	- Kronecker delta
γ	- ratio of specific heats, c_p/c_v
δ_{99}	- boundary layer thickness, value of y for which $u = 0.99 u_e$
δ_M	- value of δ_{99} for $Re_x = 10^6$
λ, Λ	- scalar measures of length
μ, μ^*	- first and second coefficients of viscosity
ρ	- density
σ	- ratio of mean density to mean temperature, $\bar{\rho}/\bar{T}$
τ_i^j	- stress tensor
ϕ	- see Eq. (6)
ψ	- see Eq. (5)

Subscripts

e	- free stream conditions
s	- derivative with respect to temperature
t	- derivative with respect to time
w	- wall conditions

Bars indicate mean values and primes indicate departures from the mean.

1. INTRODUCTION

A simple analytical model of transition was constructed by the authors in 1967 in order to study whether stream tube stretching effects might be responsible for the low Reynolds number transitions of boundary layers near the stagnation points of blunt bodies (Ref. 1). This simple model was not an invariant model and could not, therefore, form the basis for any general theory of turbulent shear layers. The model did, however, predict a number of features of actual turbulent boundary layers with sufficient accuracy to encourage its originators to undertake the development of an invariant model designed expressly for the computation of turbulent shear flows. For the case of incompressible shear layers, the development of the model was not too difficult (Ref. 2). The model for incompressible layers follows closely the pioneering work of Kolmogorov (Ref. 3), Prandtl (Ref. 4), Chou (Ref. 5) and Rotta (Ref. 6) in that it seeks a second-order closure of the equations for the mean and fluctuating velocity fields that were originally studied by Reynolds (Ref. 7).

From the inception of our work on incompressible turbulent shear flow, the ultimate goal of our efforts has been the development of a method for computing the behavior of shear layers in compressible flows. This aspect of our research efforts in turbulent modeling has been supported in its entirety by the National Aeronautics and Space Administration. In this report, we will present the results that have been obtained to date under NASA contracts NASW-1777 and NASW-2224.

This study has been limited to the case of a flat plate boundary layer where the mean pressure can be taken to be constant. Thus, we restrain somewhat the complexity of the analysis.

2. ANALYSIS

The basic equations used in this study are the following:

Continuity

$$\rho_t + (\rho u^l)_{,l} = 0 \quad (1)$$

Momentum

$$\rho u_{i,t} + \rho u^l u_{i,l} = -p_{,i} + \tau_{i,l}^l \quad (2)$$

where

$$\tau_i^j = g^{j\ell} \mu (u_{i,l} + u_{l,i}) + \delta_i^j \mu^* u_{,l}^l \quad (3)$$

Energy

$$\rho e_t + \rho u^l e_{,l} = -\rho u_{,l}^l + \psi \quad (4)$$

where

$$\psi = \phi - H \quad (5)$$

and

$$\phi = \tau_{l,m}^m u_{,m}^l \quad (6)$$

$$H = -g^{\ell m} (kT_{,l})_{,m} \quad (7)$$

The thermodynamic relations of a "calorically perfect" gas are used

$$p = \rho RT \quad (8)$$

$$e = c_v T \quad (9)$$

where R and c_v are constants.

Writing the dependent variables in these equations as the sum of a mean and fluctuating part ($\rho = \bar{\rho} + \rho'$, for example), we

can deduce equations for the mean quantities and the second-order correlations of the fluctuations by protracted manipulations. The resulting set of equations will be less formidable if we make some simplifying assumptions. They are

- 1) Fourth-order correlations are neglected.
- 2) Third-order correlations involving μ , μ^* , or k are neglected.
- 3) The fluctuations ρ' and T' are related by

$$\bar{\rho}T' + \bar{T}\rho' = 0 \quad (10)$$

- 4) The mean flow is steady.
- 5) The mean pressure is constant

$$\bar{p}_{,i} = 0 \quad (11)$$

- 6) The fluctuations in viscosity and heat conduction are related to the temperature fluctuations by the expressions

$$\begin{aligned} \mu' &= \mu_s T' \\ \mu^{*'} &= \mu_s^{*'} T' \\ k' &= k_s T' \end{aligned} \quad (12)$$

$$\begin{aligned} \mu'_{,i} &= \mu_{s,i} T'_{,i} \\ \mu^{*'}_{,i} &= \mu_{s,i}^{*'} T'_{,i} \\ k'_{,i} &= k_{s,i} T'_{,i} \end{aligned} \quad (13)$$

where the subscript s denotes a derivative with respect to temperature evaluated at \bar{T} .

The first two of these assumptions are based on the known properties of compressible turbulent boundary layers; the terms in question are at least quite small if not entirely negligible. The third assumption needs further explanation. If the mean of the equation of state

$$\bar{p} = R(\bar{\rho}\bar{T} + \overline{\rho'T'}) \quad (14)$$

is subtracted from the equation of state (8), we obtain

$$p' = R(\bar{\rho}T' + \bar{T}\rho' + \rho'T' - \overline{\rho'T'}) \quad (15)$$

Experimental evidence [Ref. 8] shows that for a boundary layer on a flat plate p'/\bar{p} is small in comparison with T'/\bar{T} and $\rho'/\bar{\rho}$. On this basis we assume that (15) is dominated by the first two terms on the right-hand side, i.e., that (10) is true, and that p' is of the order of the last two terms in (15).

The fourth and fifth assumptions are appropriate to the flat plate boundary layer flow under investigation. The sixth assumption is justifiable when the first two assumptions are valid.

The divergence of the velocity fluctuation $u'_{,l}$ is evaluated by the following steps. The equation obtained by subtracting the mean of the continuity equation from the continuity equation itself may be interpreted as the relation governing ρ' . It is linearized in the fluctuations, giving:

$$\rho'_t + \bar{u}^l \rho'_{,l} + u'_{,l} \bar{\rho} + \bar{\rho} u'_{,l} + \rho' \bar{u}^l_{,l} = 0 \quad (16)$$

A similar procedure using the energy equation yields

$$\begin{aligned} \bar{\rho} e'_t + \bar{\rho} \bar{u}^l e'_{,l} + \rho' \bar{u}^l \bar{e}_{,l} + \bar{\rho} u'_{,l} \bar{e}_{,l} &= \\ &= - \bar{\rho} u'_{,l} - p' \bar{u}^l_{,l} + \psi' \end{aligned} \quad (17)$$

Using (9) and (10) and taking into account the assumptions noted above, (16) and (17) can be combined to give

$$u'_{,l} = \frac{R}{R + c_v} \frac{\psi'}{\bar{p}} = \frac{\gamma - 1}{\gamma \bar{p}} \psi' \quad (18)$$

It is now practical to write the equations for the mean quantities and for the second-order correlations. They are

$$\begin{aligned}
\bar{\rho}\bar{u}^l\bar{u}_{i,l} - \overline{\sigma u'^l{}_{T'}}\bar{u}_{i,l} + \left(\overline{\bar{\rho}u'^l{}_{u'_i}} - \bar{u}^l\overline{\sigma u'^l{}_{T'}} - \overline{\sigma u'^l{}_{u'_i T'}} \right),l = \\
= \bar{\tau}_{i,l}^l
\end{aligned} \tag{19}$$

$$\begin{aligned}
c_v \left[\overline{\bar{\rho}\bar{u}^l{}_{T'}}_{,l} - \overline{\sigma u'^l{}_{T' T'}}_{,l} + \left(\overline{\bar{\rho}u'^l{}_{T'}} - \bar{u}^l\overline{\sigma T' T' T'} - \overline{\sigma u'^l{}_{T' T'}} \right),l \right] = \\
= -\bar{\rho}\bar{u}_{,l}^l + \bar{\psi}
\end{aligned} \tag{20}$$

$$\begin{aligned}
\bar{\rho}\bar{u}^l(\overline{u'_i u'_j}),l + \left(\overline{\bar{\rho}u'^l{}_{u'_i u'_j}} - \bar{u}^l\overline{\sigma u'^l{}_{u'_j T'}} \right),l + \left(\overline{\sigma u'^l{}_{T'}} \right),l \overline{u'_i u'_j} \\
= \overline{\sigma u'^l{}_{T' i}}\bar{u}_{i,l} - \overline{\sigma u'^l{}_{T' j}}\bar{u}_{j,l} + \overline{u'^l{}_{u'_j}}\bar{\rho}\bar{u}_{i,l} \\
+ \overline{u'^l{}_{u'_i}}\bar{\rho}\bar{u}_{j,l} - \overline{\sigma u'^l{}_{u'_j T' i}}\bar{u}_{i,l} - \overline{\sigma u'^l{}_{u'_i T' j}}\bar{u}_{j,l} = \\
= -(\overline{u'_j p'})_{,i} - (\overline{u'_i p'})_{,j} \\
+ \overline{p' u'_{j,i}} + \overline{p' u'_{i,j}} + \overline{u'_j \tau'_{i,l}} + \overline{u'_i \tau'_{j,l}}
\end{aligned} \tag{21}$$

$$\begin{aligned}
c_v \left[\overline{\bar{\rho}\bar{u}^l{}_{(T' T')}}_{,l} + \left(\overline{\bar{\rho}u'^l{}_{T' T'}} - \bar{u}^l\overline{\sigma T' T' T'} \right),l \right. \\
+ \left(\overline{\sigma u'^l{}_{T'}} \right),l \overline{T' T'} - 2\overline{\sigma T' T' i}\bar{u}^l{}_{T'},l \\
\left. + 2\overline{u'^l{}_{T' i}}\bar{\rho}\bar{T}_{,l} - 2\overline{\sigma u'^l{}_{T' T' T'}}_{,l} \right] = \\
= \frac{2}{\gamma} \overline{T' \psi'} - 2\overline{p' T' i}\bar{u}_{,l}^l
\end{aligned} \tag{22}$$

$$\begin{aligned}
c_v \left[\overline{\bar{\rho} \bar{u}^\ell (u_i^{T'})}, \ell + \left(\overline{\bar{\rho} u_i^{T'} u_i^{T'}} - \bar{u}^\ell \overline{\sigma u_i^{T'} T'} \right), \ell + \left(\overline{\sigma u_i^{T'} T'} \right), \ell \overline{u_i^{T'}} \right. \\
- \overline{\sigma u_i^{T'} \bar{u}^\ell T'}, \ell - \overline{\sigma T' T' \bar{u}^\ell \bar{u}_i}, \ell + \overline{u_i^{T'} u_i^{T'} \bar{\rho} T'}, \ell \\
\left. + \overline{u_i^{T'} \bar{\rho} \bar{u}_i}, \ell - \overline{\sigma u_i^{T'} u_i^{T'} T'}, \ell - \overline{\sigma u_i^{T'} T' T' \bar{u}_i}, \ell \right] = \\
= \frac{1}{\gamma} \overline{u_i^{T'} \psi'} - \overline{u_i^{T'} \rho' \bar{u}^\ell}, \ell - c_v \overline{(\rho' T')}, i \\
+ c_v \overline{\rho' T'}, i + c_v \overline{T' \tau_{i, \ell}^\ell} \quad (23)
\end{aligned}$$

In these equations,

$$\sigma = \bar{\rho} / \bar{T} \quad (24)$$

$$\bar{\tau}_i^j = g^{j\ell} \left[\bar{\mu} (\bar{u}_{i, \ell} + \bar{u}_{\ell, i}) + \mu_s \left(\overline{T' u_{i, \ell}'} + \overline{T' u_{\ell, i}'} \right) \right] + \delta_i^j \bar{\mu}^* \bar{u}^\ell, \ell \quad (25)$$

$$\bar{\psi} = \bar{\phi} - \bar{H}, \quad \psi' = \phi' - H' \quad (26)$$

$$\begin{aligned}
\bar{\phi} = \bar{\tau}_{\ell, m}^m \bar{u}^\ell + \bar{\mu} \left[g^{mn} \overline{u_{\ell, n}' u_{m, \ell}'} + \left(\overline{u_i^{T'} u_i^{T'}}, \ell, m \right) \right. \\
\left. + \mu_s g^{mn} (\bar{u}_{\ell, n} + \bar{u}_{n, \ell}) \overline{T' u_{m, \ell}'} \right] \quad (27)
\end{aligned}$$

$$\bar{H} = - g^{\ell m} \left[\left(\overline{\bar{k} T'}, \ell \right), m + k_s \overline{(T' T')}, \ell, m \right] \quad (28)$$

$$\begin{aligned}
\overline{u_j^{T'} \tau_{i, \ell}^\ell} + \overline{u_i^{T'} \tau_{j, \ell}^\ell} = g^{\ell m} \left[\left(\bar{\mu} \overline{(u_i^{T'} u_j^{T'})}, m \right), \ell - 2 \bar{\mu} \overline{u_{j, m}' u_{i, \ell}'} \right] \\
+ 2 \bar{\mu}_{, \ell} \left(\overline{u_j^{T'} u_{i, \ell}'} + \overline{u_i^{T'} u_{j, \ell}'} \right) \\
+ \mu_s g^{\ell m} \left\{ \left[\left(\bar{u}_{i, m} + \bar{u}_{m, i} \right) \overline{u_j^{T'}}, \ell \right] \right. \\
+ \left[\left(\bar{u}_{j, m} + \bar{u}_{m, j} \right) \overline{u_i^{T'}}, \ell \right] - \left(\bar{u}_{i, m} + \bar{u}_{m, i} \right) \overline{T' u_{j, \ell}'} \\
\left. - \left(\bar{u}_{j, m} + \bar{u}_{m, j} \right) \overline{T' u_{i, \ell}'} \right\} + \mu_s^* \left[\left(\bar{u}_{, m}^m \overline{u_j^{T'}}, i \right) \right. \\
\left. + \left(\bar{u}_{, m}^m \overline{u_i^{T'}}, j \right) - \bar{u}_{, m}^m \left(\overline{T' u_{j, i}'} + \overline{T' u_{i, j}'} \right) \right] \quad (29)
\end{aligned}$$

$$\begin{aligned}
\overline{T' \tau'_{i,l}} &= g^{lm} \overline{\mu_{T' u'_{i,m,l}}} + \mu_s \left\{ \overline{T',l} \left(g^{lm} \overline{T' u'_{i,m}} + \overline{T' u'_{i,l}} \right) \right. \\
&+ g^{lm} \left[\left(\overline{u'_{i,m}} + \overline{u'_{m,i}} \right) \overline{T' T'} \right], l \\
&+ g^{lm} \left(\overline{u'_{i,m,l}} + \overline{u'_{m,i,l}} \right) \overline{T' T'} \left. \right\} \\
&+ \frac{1}{2} \mu_s^* \left[\left(\overline{u'_{m,i}} \right) \overline{T' T'} \right], i + \overline{u'_{m,i}} \overline{T' T'} \left. \right] \quad (30)
\end{aligned}$$

$$\begin{aligned}
\overline{u'_{i,l} \phi'} &= \overline{\tau'_{l,i} u'_{i,m}} + \overline{u'_{m,l}} \left[\overline{\mu} \left(g^{mn} \overline{u'_{i,l,n}} + \overline{u'_{i,l} u'_{n,m}} \right) \right. \\
&+ \mu_s g^{mn} \overline{u'_{i,T'}} \left(\overline{u'_{l,n}} + \overline{u'_{n,l}} \right) \left. \right] + \mu_s^* \overline{u'_{l,m}} \overline{u'_{i,T'}} \quad (31)
\end{aligned}$$

$$\begin{aligned}
\overline{T' \phi'} &= \overline{\tau'_{l,T'} u'_{i,m}} + \overline{u'_{m,l}} \left[\overline{\mu} \left(g^{mn} \overline{T' u'_{l,n}} + \overline{T' u'_{l,m}} \right) \right. \\
&+ \mu_s g^{mn} \overline{T' T'} \left(\overline{u'_{l,n}} + \overline{u'_{n,l}} \right) \left. \right] + \mu_s^* \overline{u'_{l,m}} \overline{T' T'} \quad (32)
\end{aligned}$$

$$\begin{aligned}
- \overline{u'_{i,l} H'} &= \overline{k g^{lm} u'_{i,T',l,m}} + k_s g^{lm} \left[\overline{u'_{i,T',l,m}} + 2 \overline{T',l} \left(\overline{u'_{i,T'}} \right) \right. \\
&- \left. 2 \overline{T',l} \overline{T' u'_{i,m}} \right] \quad (33)
\end{aligned}$$

$$- \overline{T' H'} = \frac{1}{2} \overline{k g^{lm}} \left[\left(\overline{T' T'} \right) \right], l, m - 2 \overline{T',l} \overline{T',m} \left. \right] + k_s g^{lm} \left(\overline{T' T' T'} \right), l, m \quad (34)$$

We now display the models used to close the above-listed set of equations. As in Ref. 2, we set

$$\overline{p' u'_{j,i}} + \overline{p' u'_{i,j}} = - \overline{\rho} \frac{q}{\Lambda} \left(\overline{u'_{i,j}} - \frac{1}{3} g_{ij} K \right) \quad (35)$$

where

$$q^2 \equiv K \equiv \overline{u'_{i,l} u'_{l,i}} \quad (36)$$

and Λ (Λ_1 in Ref. 2) is a scalar length to be determined.

To the same order that (10) is justified, it is unnecessary to modify (35) for the effect of nonzero divergence of the turbulent velocity field. By analogy with (35), we write

$$\overline{p'T',i} = -\frac{1-\rho}{2\rho p_T} \frac{q}{\Lambda} \overline{u_i'T'} \quad (37)$$

where p_T is a dimensionless parameter.

Again following Ref. 2, we write

$$\overline{u_i'u_j'u_k'} = -V_C \Lambda q \left[(\overline{u_i'u_j'})_{,k} + (\overline{u_j'u_k'})_{,i} + (\overline{u_k'u_i'})_{,j} \right] \quad (38)$$

where V_C is a dimensionless parameter. (In Ref. 2, Λ_2 represents $V_C \Lambda$.) Analogously we set

$$\overline{u_i'u_j'T'} = -V_{VT} \Lambda q \left[(\overline{u_i'T'})_{,j} + (\overline{u_j'T'})_{,i} \right] \quad (39)$$

$$\overline{u_i'T'T'} = -V_{TT} \Lambda q (\overline{T'T'})_{,i} \quad (40)$$

where V_{VT} and V_{TT} are dimensionless parameters.

In accord with the approximation (10), we model

$$\overline{u_i'p'} = 0 \quad (41)$$

This corresponds to setting $\Lambda_3 = 0$ in Ref. 2. By analogy,

$$\overline{p'T'} = 0 \quad (42)$$

We also set

$$\overline{T'T'T'} = 0 \quad (43)$$

From Ref. 2 once more

$$\overline{u_{i,m}'u_{j,n}'} = \frac{g_{mn}}{3} \frac{\overline{u_i'u_j'}}{\lambda^2} \quad (44)$$

Analogously,

$$\overline{u_{i,m}'T'_{,n}} = \frac{g_{mn}}{3} \frac{\overline{u_i'T'}}{\lambda^2} \quad (45)$$

$$\overline{T'_{,m}T'_{,n}} = \frac{g_{mn}}{3} \frac{\overline{T'T'}}{\lambda^2} \quad (46)$$

In these models, λ is another scalar length to be determined.

We also set

$$\overline{u_i' u_j'} = \frac{1}{2} (\overline{u_i' u_j'})_{,k} \quad (47)$$

$$\overline{T' u_{i,j}'} = \frac{1}{3} g_{ij} \overline{T' u_{,l}'} \quad (48)$$

As mentioned above, many of the models are taken from Ref. 2. Most of the others are similar to models we have used in studies of atmospheric turbulence [Ref. 9]. The models (43), (47), and (48) are new to this study.

Using the notation

$$S_V = q/\Lambda \quad (49)$$

$$S_T = p_T q/\Lambda \quad (50)$$

we substitute from (25) through (50) back into (19) through (23) to obtain the following set

$$\begin{aligned} \bar{\rho} \bar{u}^{\ell} \bar{u}_{i,l} - \overline{\sigma u_i'^{\ell} T' \bar{u}_{i,l}} + \left[\overline{\bar{\rho} u_i'^{\ell} u_i'} - \overline{\sigma \bar{u}^{\ell} u_i' T'} \right. \\ \left. + V_{VT} \Lambda q \sigma g^{\ell m} \left((\overline{u_i' T'})_{,m} + (\overline{u_m' T'})_{,i} \right) \right]_{,l} \\ = g^{\ell m} \left(\bar{\mu} (\bar{u}_{i,m} + \bar{u}_{m,i}) \right)_{,l} + (\bar{\mu}^* \bar{u}^{\ell})_{,l}, i \end{aligned} \quad (51)$$

$$\begin{aligned} \bar{\rho} \bar{u}^{\ell} \bar{T}_{,l} - \overline{\sigma u_i'^{\ell} T' \bar{T}_{,l}} + \left[\overline{\bar{\rho} u_i'^{\ell} T'} - \overline{\sigma \bar{u}^{\ell} T' T'} + V_{TT} \Lambda q \sigma g^{\ell m} (\overline{T' T'})_{,m} \right]_{,l} \\ = -\frac{1}{c_V} \bar{p} \bar{u}^{\ell}_{,l} + \frac{1}{c_V} \left\{ \bar{\mu} \left[g^{mn} (\bar{u}_{l,n} + \bar{u}_{n,l}) \bar{u}^{\ell}_{,m} \right. \right. \\ \left. \left. + (\overline{u_i'^{\ell} u_i'^m})_{,l,m} + \frac{u_i'^{\ell} u_{l,i}'}{\lambda^2} \right] + \bar{\mu}^* \bar{u}^{\ell}_{,l} \bar{u}^m_{,m} \right. \\ \left. + g^{\ell m} \left[(\bar{k} \bar{T}_{,l})_{,m} + \frac{1}{2} k_s (\overline{T' T'})_{,l,m} \right] \right\} \end{aligned} \quad (52)$$

c

$$\begin{aligned}
\bar{\rho}\bar{u}^{\ell}(\bar{u}'_i\bar{u}'_j)_{,l} &= g^{\ell m} \left[V_C \bar{\rho} \Lambda q \left((\bar{u}'_i\bar{u}'_j)_{,m} + (\bar{u}'_j\bar{u}'_m)_{,i} + (\bar{u}'_m\bar{u}'_i)_{,j} \right) \right]_{,l} \\
&+ \left[V_{VT} \bar{u}^{\ell} \Lambda q \sigma \left((\bar{u}'_i\bar{T}'_i)_{,j} + (\bar{u}'_j\bar{T}'_i)_{,i} \right) \right]_{,l} \\
&+ \left(\overline{\sigma u'^{\ell} T'_i} \right)_{,l} \bar{u}'_i\bar{u}'_j - \overline{\sigma u'_i T'_i} \bar{u}^{\ell} \bar{u}_{j,l} - \overline{\sigma u'_j T'_i} \bar{u}^{\ell} \bar{u}_{i,l} \\
&+ \bar{\rho} \overline{u'^{\ell} u'_i} \bar{u}_{i,l} + \bar{\rho} \overline{u'^{\ell} u'_j} \bar{u}_{i,l} \\
&+ V_{VT} \Lambda q \sigma g^{\ell m} \left[\left((\bar{u}'_m\bar{T}'_i)_{,i} + (\bar{u}'_i\bar{T}'_i)_{,m} \right) \bar{u}_{j,l} \right. \\
&\left. + \left((\bar{u}'_m\bar{T}'_i)_{,j} + (\bar{u}'_j\bar{T}'_i)_{,m} \right) \bar{u}_{i,l} \right] \\
&= -\bar{\rho} S_V \left(\bar{u}'_i\bar{u}'_j - \frac{1}{3} g_{ij} K \right) + g^{\ell m} \left(\bar{\mu}(\bar{u}'_i\bar{u}'_j)_{,l} \right)_{,m} \\
&- 2\bar{\mu} \frac{\bar{u}'_i\bar{u}'_j}{\lambda^2} + \mu_S \bar{T}_{,l} \left((\bar{u}'^{\ell} \bar{u}'_i)_{,j} + (\bar{u}'^{\ell} \bar{u}'_j)_{,i} \right) \\
&+ \mu_S g^{\ell m} \left[\bar{u}'_i\bar{T}'_i (\bar{u}_{j,m} + \bar{u}_{m,j}) + \bar{u}'_j\bar{T}'_i (\bar{u}_{i,m} + \bar{u}_{m,i}) \right]_{,l} \\
&+ \mu_S^* \left[(\bar{u}'_i\bar{T}'_i \bar{u}^m_{,m})_{,j} + (\bar{u}'_j\bar{T}'_i \bar{u}^m_{,m})_{,i} \right] \quad (53)
\end{aligned}$$

$$\begin{aligned}
\bar{\rho}\bar{u}^{\ell}(\bar{T}'_i\bar{T}'_i)_{,l} &= g^{\ell m} \left(V_{TT} \bar{\rho} \Lambda q (\bar{T}'_i\bar{T}'_i)_{,m} \right)_{,l} + (\overline{\sigma u'^{\ell} T'_i})_{,l} \bar{T}'_i\bar{T}'_i \\
&- 2\sigma \bar{T}'_i\bar{T}'_i \bar{u}^{\ell} \bar{T}_{,l} + 2\bar{\rho} \overline{u'^{\ell} T'_i} \bar{T}_{,l} + 2g^{\ell m} V_{TT} \Lambda q \sigma (\bar{T}'_i\bar{T}'_i)_{,m} \bar{T}_{,l} \\
&= \frac{2}{c_p} \left(\mu_S g^{mn} \bar{u}^{\ell}_{,m} (\bar{u}_{\ell,n} + \bar{u}_{n,\ell}) + \mu_S^* \bar{u}^{\ell}_{,l} \bar{u}^m_{,m} \right) \bar{T}'_i\bar{T}'_i \\
&+ \frac{1}{c_p} \left[\bar{k} g^{\ell m} (\bar{T}'_i\bar{T}'_i)_{,l,m} - 2\bar{k} \frac{\bar{T}'_i\bar{T}'_i}{\lambda^2} \right. \\
&\left. + 2k_S g^{\ell m} (\bar{T}'_i\bar{T}'_i \bar{T}'_i)_{,l,m} \right] \quad (54)
\end{aligned}$$

$$\begin{aligned}
& \bar{\rho} \bar{u}^{\ell}(\bar{u}'_{iT'})_{,l} - g^{\ell m} \left[V_{VT} \bar{\rho} \Lambda q \left((\bar{u}'_{iT'})_{,m} + (\bar{u}'_{mT'})_{,i} \right) \right]_{,l} \\
& + \left[V_{TT} \Lambda q \sigma \bar{u}^{\ell}(\bar{T}'T')_{,i} \right]_{,l} + (\sigma u'^{\ell T'})_{,l} \bar{u}'_{iT'} \\
& - \sigma \bar{T}'T' \bar{u}^{\ell} \bar{u}'_{i,l} - \sigma \bar{u}'_{iT'} \bar{u}^{\ell} \bar{T}'_{,l} \\
& + \bar{\rho} u'^{\ell T'} \bar{u}'_{i,l} + \bar{\rho} u'^{\ell} u'_{iT'} \bar{T}'_{,l} + V_{TT} \Lambda q \sigma g^{\ell m} (\bar{T}'T')_{,m} \bar{u}'_{i,l} \\
& + V_{VT} \Lambda q \sigma g^{\ell m} \left((\bar{u}'_{iT'})_{,m} + (\bar{u}'_{mT'})_{,i} \right) \bar{T}'_{,l} \\
& = \frac{1}{c_p} \bar{\mu} \left[\left(g^{kl} \bar{u}'_{,k} + g^{mn} \bar{u}'_{,m} \right) (\bar{u}'_{i'n'})_{,l} \right] \\
& + \frac{1}{c_p} \left[\mu_s g^{mn} \bar{u}'_{,m} (\bar{u}'_{l,n} + \bar{u}'_{n,l}) + \mu_s^* \bar{u}'_{,l} \bar{u}'_{,m} \right] \bar{u}'_{iT'} \\
& + \frac{1}{c_p} \left[g^{\ell m} \left(\bar{k}(\bar{u}'_{iT'})_{,m} \right)_{,l} - \bar{k} \frac{\bar{u}'_{iT'}}{\lambda^2} + k_s g^{\ell m} (\bar{u}'_{iT'} \bar{T}'_{,l})_{,m} \right] \\
& - \frac{1}{2} \bar{\rho} S_T \bar{u}'_{iT'} - \bar{\mu} \frac{\bar{u}'_{iT'}}{\lambda^2} \\
& + \mu_s g^{\ell m} \left[(\bar{T}'T'(\bar{u}'_{i,m} + \bar{u}'_{m,i}))_{,l} + \bar{T}'T'(\bar{u}'_{i,m} + \bar{u}'_{m,i})_{,l} \right] \\
& + \frac{1}{2} \mu_s^* \left[(\bar{T}'T' \bar{u}'_{,m})_{,i} + \bar{T}'T' \bar{u}'_{,m,i} \right] \tag{55}
\end{aligned}$$

In these equations, $\bar{\mu}$, $\bar{\mu}^*$, \bar{k} , μ_s , μ_s^* , and k_s are known functions of \bar{T} ; $\bar{\rho}$ is a known constant; and from (14) and (10)

$$\bar{\rho} = \frac{\bar{\rho}}{R(\bar{T} - \bar{T}'T'/\bar{T})} \tag{56}$$

After nondimensionalizing the equations, we next expand them by inserting numerical values for the free indices and implementing the summation convention. This task was accomplished by the computer program TENSUR which was developed for this project under NASA Contract NASW-1777. The resulting equations were then

reduced to their two-dimensional boundary layer form. In terms of the Cartesian coordinates x, y, z (instead of x_1, x_2, x_3) and the velocity components u, v, w (instead of u_1, u_2, u_3), the criteria used for dropping terms were

$$\bar{w} = 0 \quad (57)$$

$$\frac{\partial}{\partial z} = 0 \quad (58)$$

$$\bar{v} \ll \bar{u} \quad (59)$$

$$\frac{\partial}{\partial x} \ll \frac{\partial}{\partial y} \quad (60)$$

but with $\bar{u}\partial/\partial x$ the same order as $\bar{v}\partial/\partial y$. In the resulting equations, it can be observed that there is no production term for $\overline{v'w'}$ and that the only production terms for $\overline{u'w'}$ and $\overline{w'T'}$ contain the factor $\overline{v'w'}$. In addition, none of the other unknowns depend on $\overline{v'w'}$, $\overline{u'w'}$, or $\overline{w'T'}$ in any way. We, therefore, no longer consider these three quantities or the equations governing them.

The resulting set of equations then becomes the following:

$$\bar{\rho}\bar{u}\bar{u}_x + \bar{\rho}\bar{v}\bar{u}_y - \overline{\sigma v'T'u_y} + (\overline{\rho u'v'})_y + (V_{VT}\sigma\Lambda q(\overline{u'T'})_y)_y = (\bar{\mu}\bar{u}_y)_y \quad (61)$$

$$\begin{aligned} & \bar{\rho}\bar{u}\bar{T}_x + \bar{\rho}\bar{v}\bar{T}_y - \overline{\sigma v'T'T_y} + (\overline{\rho v'T'})_y + (V_{TT}\sigma\Lambda q(\overline{T'T'})_y)_y \\ & = -(\gamma - 1)(\bar{u}_x + \bar{v}_y) + \gamma(\gamma - 1)M_e^2 \cdot \\ & \cdot \bar{\mu} \left[\bar{u}_y^2 + (\overline{v'v'})_{yy} + \frac{K}{\lambda^2} \right] \\ & + \gamma(\overline{kT}_y)_y + \frac{\gamma}{2} k_s (\overline{T'T'})_{yy} \end{aligned} \quad (62)$$

$$\begin{aligned}
& \bar{\rho}\bar{u}(\overline{u'u'})_x + \bar{\rho}\bar{v}(\overline{u'u'})_y + 2\bar{\rho}\overline{v'u'}\bar{u}_y - (V_C\bar{\rho}\Lambda q(\overline{u'u'})_y)_y \\
& + C_{UU}\overline{u'u'} - \frac{1}{3}\bar{\rho}S_V(\overline{v'v'} + \overline{w'w'}) \\
& - 2\sigma\overline{u'T'}(\bar{u}\bar{u}_x + \bar{v}\bar{u}_y) + 2V_{VT}\sigma\Lambda q(\overline{u'T'})_y\bar{u}_y \\
& = (\bar{\mu}(\overline{u'u'})_y)_y + 2\mu_S(\overline{u'T'}\bar{u}_y)_y
\end{aligned} \tag{63}$$

$$\begin{aligned}
& \bar{\rho}\bar{u}(\overline{v'v'})_x + \bar{\rho}\bar{v}(\overline{v'v'})_y - 3(V_C\bar{\rho}\Lambda q(\overline{v'v'})_y)_y + C_{UU}\overline{v'v'} \\
& - \frac{1}{3}\bar{\rho}S_V(\overline{u'u'} + \overline{w'w'}) \\
& = (\bar{\mu}(\overline{v'v'})_y)_y + 2\mu_S\bar{T}_y(\overline{v'v'})_y
\end{aligned} \tag{64}$$

$$\begin{aligned}
& \bar{\rho}\bar{u}(\overline{w'w'})_x + \bar{\rho}\bar{v}(\overline{w'w'})_y - (V_C\bar{\rho}\Lambda q(\overline{w'w'})_y)_y + C_{UU}\overline{w'w'} \\
& - \frac{1}{3}\bar{\rho}S_V(\overline{u'u'} + \overline{v'v'}) \\
& = (\bar{\mu}(\overline{w'w'})_y)_y
\end{aligned} \tag{65}$$

$$\begin{aligned}
& \bar{\rho}\bar{u}(\overline{u'v'})_x + \bar{\rho}\bar{v}(\overline{u'v'})_y + \bar{\rho}\overline{v'v'}\bar{u}_y - 2(V_C\bar{\rho}\Lambda q(\overline{u'v'})_y)_y \\
& + C_{UV}\overline{u'v'} - \sigma\overline{v'T'}(\bar{u}\bar{u}_x + \bar{v}\bar{u}_y) + 2V_{VT}\sigma\Lambda q(\overline{v'T'})_y\bar{u}_y \\
& = (\bar{\mu}(\overline{u'v'})_y)_y + \mu_S\bar{T}_y(\overline{u'v'})_y + \mu_S(\overline{v'T'}\bar{u}_y)_y
\end{aligned} \tag{66}$$

$$\begin{aligned}
& \bar{\rho}\bar{u}(\overline{T'T'})_x + \bar{\rho}\bar{v}(\overline{T'T'})_y + 2\bar{\rho}\overline{v'T'}\bar{T}_y - (V_{TT}\bar{\rho}\Lambda q(\overline{T'T'})_y)_y \\
& + C_{TT}\overline{T'T'} - 2\sigma\overline{T'T'}(\bar{u}\bar{T}_x + \bar{v}\bar{T}_y) + 2V_{TT}\sigma\Lambda q(\overline{T'T'})_y\bar{T}_y \\
& = \bar{k}((\overline{T'T'})_y)_y + 2k_S(\overline{T'T'}\bar{T}_y)_y
\end{aligned} \tag{67}$$

$$\begin{aligned}
& \bar{\rho}\bar{u}(\overline{u'T'})_x + \bar{\rho}\bar{v}(\overline{u'T'})_y + \bar{\rho}(\overline{v'T'}\bar{u}_y + \overline{u'v'T'}) - (V_{VT}\bar{\rho}\Lambda q(\overline{u'T'})_y)_y \\
& + C_{UT}\overline{u'T'} - \overline{\sigma T'T'}(\bar{u}\bar{u}_x + \bar{v}\bar{u}_y) - \overline{\sigma u'T'}(\bar{u}\bar{T}_x + \bar{v}\bar{T}_y) \\
& + \sigma\Lambda q(V_{TT}(\overline{T'T'})_y\bar{u}_y + V_{VT}(\overline{u'T'})_y\bar{T}_y) \\
& = (\gamma - 1)M_e^2\bar{\mu}(\overline{u'u'})_y\bar{u}_y + (\bar{k}(\overline{u'T'})_y)_y \\
& + k_s(\overline{u'T'T'})_y + \mu_s(\overline{T'T'}\bar{u}_y)_y + \mu_s\overline{T'T'}\bar{u}_{yy} \tag{68}
\end{aligned}$$

$$\begin{aligned}
& \bar{\rho}\bar{u}(\overline{v'T'})_x + \bar{\rho}\bar{v}(\overline{v'T'})_y + \bar{\rho}\overline{v'v'T'} - 2(V_{VT}\bar{\rho}\Lambda q(\overline{v'T'})_y)_y \\
& + C_{UT}\overline{v'T'} - \overline{\sigma v'T'}(\bar{u}\bar{T}_x + \bar{v}\bar{T}_y) + 2\sigma\Lambda qV_{VT}(\overline{v'T'})_y\bar{T}_y \\
& = (\gamma - 1)M_e^2\bar{\mu}(\overline{u'v'})_y\bar{u}_y + (\bar{k}(\overline{v'T'})_y)_y + k_s(\overline{v'T'T'})_y \tag{69}
\end{aligned}$$

The mean of the continuity equation is appended to these equations, i.e.,

$$(\bar{\rho}\bar{u})_x + (\bar{\rho}\bar{v})_y - (\overline{\sigma v'T'})_y = 0 \tag{70}$$

which is used to determine \bar{v} since the equation for the momentum in the y direction is not useful for determining \bar{v} in a boundary layer.

The following new symbols appear in (61) through (69):

$$C_{UU} = (\overline{\sigma v'T'})_y + \frac{2\bar{\mu}}{\lambda^2} + \frac{2}{3}\bar{\rho}S_V \tag{71}$$

$$C_{UV} = (\overline{\sigma v'T'})_y + \frac{2\bar{\mu}}{\lambda^2} + \bar{\rho}S_V \tag{72}$$

$$C_{TT} = (\overline{\sigma v'T'})_y + \frac{2\bar{k}}{\lambda^2} - 2(\gamma - 1)M_e^2\mu_s\bar{u}_y^2 \tag{73}$$

$$C_{UT} = (\overline{\sigma v'T'})_y + \frac{\bar{\mu} + \bar{k}}{\lambda^2} + \frac{1}{2}\bar{\rho}S_T - (\gamma - 1)M_e^2\mu_s\bar{u}_y^2 \tag{74}$$

M_e is the Mach number of the free stream and enters the equations in the process of making them nondimensional. The viscosity μ has been made nondimensional by dividing it by $\rho_e u_e L$ where L is the reference length. Similarly, k has been made nondimensional by dividing by $c_p \rho_e u_e L$. Note that, under the boundary layer and modeling assumptions, the second coefficient of viscosity μ^* has dropped from the equations entirely.

3. NUMERICAL STUDY

The numerical integration of Eqs. (61) through (69) was performed by an implicit finite-difference method. In this scheme, nonlinear terms are handled by arbitrarily evaluating a portion of such terms at the known position value, leaving a linear factor containing one of the unknowns. For this system of nine equations in nine unknowns, each element of the tridiagonal matrix which arises in the application of the implicit method is itself a nine \times nine matrix. The process of writing Fortran statements to evaluate the elements of these matrices was largely accomplished by a computer program called DIFFR which was also developed for this project under Contract No. NASW-1777.

The program that performed the numerical integration of the finite-difference equations was debugged on the IBM 1130 at A.R.A.P. Rental time on a META-4 facility was used for actual program execution.

The values of the parameters that have been found successful in previous numerical studies (Ref. 2) were used. Accordingly, Λ was set equal to the smaller of $0.7y$ and $0.15\delta_{99}$, where $\delta_{99}(x)$ is the value of y for which $\bar{u} = 0.99 u_e$; λ was determined from

$$\lambda^2 = \frac{\Lambda^2}{a + b\bar{p}q\Lambda/\bar{\mu}}$$

where $a = 2.5$ and $b = 0.125$, and V_c was set equal to 0.1 . As a first approximation, we set $V_{VT} = 0.1$, $V_{TT} = 0.1$, and $P_T = 1.0$ since these parameters did not appear in the earlier studies.

The viscosity was determined by the Sutherland law with the constant equal to 114°C . The Prandtl number was taken as 0.71 . A free stream temperature of -55°C and $\gamma = 1.4$ were used. The initial conditions on \bar{u} and \bar{T} as functions of y were approximately the laminar profiles appropriate to the given Mach number,

Reynolds number, and wall cooling conditions. The turbulent correlations $\overline{u'u'}$, $\overline{v'v'}$ and $\overline{w'w'}$ were given small initial values (the maximum for each was 10^{-5} relative to u_e^2) in a "spot" of turbulence extending from about $y = 0.2\delta_{99}$ to $y = 0.6\delta_{99}$. The other turbulent correlations were set to zero.

Five full runs were executed, with the remaining parameters varied according to the following table.

$\underline{Re_{xi}}$	$\underline{Re_{xf}}$	$\underline{M_e}$	$\underline{G_w}$
2×10^4	10^7	0	1.0
2×10^4	10^7	0	0.8
10^5	3×10^7	3	1.0
5×10^5	2×10^8	6	1.0
5×10^5	10^7	6	0.8

Here, Re_{xi} and Re_{xf} represent the initial and final values of the Reynolds number based on x ; M_e is the free stream Mach number and G_w is the ratio of the wall temperature to the free stream stagnation temperature.

In Fig. 1, we show the curves of local skin friction coefficient, c_f , versus Reynolds number for the five runs. The values and trends follow previous experimental and theoretical work.

In Fig. 2, we show the heat transfer at the wall as a function of Reynolds number for the two $M_e = 6$ cases. Since the heat transfer is negligible for $G_w = 0.8$, we assume that case represents an adiabatic wall. The recovery factor is, therefore,

$$r = \frac{T_{aw} - T_e}{T_e^0 - T_e} = \frac{0.8 \times 8.2 - 1}{8.2 - 1} = 0.77$$

This is considerably lower than the usually accepted value of about 0.89.

Knowing the adiabatic wall temperature, the Stanton number for the other $M_e = 6$ case can be determined. In Fig. 3, we show the variation of S_t along with the Reynolds analogy factor, $2S_t/c_f$. Again, there is considerable discrepancy between these values and those generally reported in the literature. For example, although there is considerable scatter in the data presented in Ref. 10, the values of the Reynolds analogy factor given there are almost all below 1.3.

For the Mach number zero case, the adiabatic wall temperature is the free stream temperature and the recovery factor is indeterminate. The Stanton number can be calculated for the case $G_w = 0.8$ and is found to range from 1.24 to 1.32, again somewhat high.

These results concerning recovery factor and Stanton number indicate that some adjustment of the model parameters is in order. As was mentioned above, there was no precedent to establish values for V_{VT} , V_{TT} , and P_T , so it is not surprising that the values chosen were somewhat off the mark.

Profiles of the dependent variables for the case $M_e = 6$, $G_w = 0.8$ at $Re_x = 10$ million are shown in Figs. 4-6. It appears that \bar{T} has a high slope at the wall but, as will be shown below, this is not the case; the change in slope cannot be represented at the scale of Fig. 4. With regard to the small hump in the \bar{v} profile near the outer edge, it may be worth remarking that the hump does not exist in a plot of $\bar{p}\bar{v}$ which increases smoothly with y .

The profiles of $\overline{v'v'}$ and $\overline{w'w'}$ are nearly identical except that the peak value of $\overline{w'w'}$ is a little higher, but $\overline{v'v'}$ spreads a little farther at the outer edge. Both these effects are easily explained by the factor 3 in the velocity diffusion term for $\overline{v'v'}$ in (64), whereas the corresponding term in (65) for $\overline{w'w'}$ has the factor 1.

Figures 7-11 show the development of the profiles through

and past transition for \bar{u} , \bar{v} , \bar{T} , $\overline{u'v'}$ and $\overline{u'T'}$ (the latter two being fairly typical of all the correlations), still for the case $M_e = 6$ and $G_w = 0.8$. It should be noted that δ_{99} , the quantity used to normalize the ordinate in those plots, varies widely as a function of Re_x as shown in Fig. 12. Also, in that figure, the curve of c_f vs. Re_x for this case is repeated and the values of Re_x for which profiles are plotted in Figs. 7-11 are indicated. It is of interest that there is a stage early in transition where \bar{v} is negative for all y and δ_{99} stops growing.

A different perspective on transition is obtained if the profiles are all plotted with the same y scaling. This is done in Figs. 13-17. For the larger Reynolds numbers, of course, only a portion of the profile is shown. In Fig. 13, it is seen that $\partial\bar{u}/\partial y$ at the wall increases and then decreases as the Reynolds number increases - the same effect seen in the c_f curve (Fig. 12).

In Fig. 15, it is clear that $\partial\bar{T}/\partial y$ at the wall does, indeed, stay close to zero for this case, in contrast to the apparent slope for high Reynolds numbers in Figs. 4 and 9.

This whole group of profiles shows that changes in conditions close to the wall are relatively slow, compared to the impression one might get from Figs. 7-11.

In Figs. 18-22, profiles are presented for all five cases at a Reynolds number of ten million. In order for the temperatures and temperature fluctuations to be comparable among the cases, we have normalized them by dividing by $T_w - T_e$ rather than T_e . Hence, the case $M_e = 0$, $G_w = 1$ (for which $T_w = T_0^0 = T_e$) is omitted from Figs. 20 and 22.

These sets of profiles illustrate the quantity of detail available from the computer runs. It should be emphasized that the curves demonstrate the behavior of our model. The relationship between the details shown and those of real flows is yet to be established.

4. SUMMARY AND CONCLUSIONS

A simplified set of equations for the means and second-order correlations in a compressible turbulent flow at constant pressure has been derived. The set has been closed using the principles of invariant modeling and further simplified by boundary-layer assumptions. Finally, the equations have been written in finite-difference form and solved numerically.

Five cases, representing different Mach numbers and wall temperatures, have been run using one set of values for the parameters introduced in the modeling. The results are very encouraging since they show many of the characteristics of real compressible boundary layers and are quantitatively correct.

We feel that this study should be continued along two lines. First, more runs should be made with the current program to understand in more detail the balances involved in the model in order to determine those changes required to improve results. Second, work should begin on the extension of the model to cases where the mean pressure is not a constant.

We thank John Yates, Barry Gilligan and Milton Teske for their contributions to this study, the staff of the Management Science Department of Batten, Barton, Durstine and Osborn for their cooperation in sharing their computer, and Sylvia Harrington for her excellent typing.

REFERENCES

1. Donaldson, Coleman duP.: "A Computer Study of an Analytical Model of Boundary Layer Transition," AIAA Journal 7, 2, (1969), pp. 272-278.
2. Donaldson, Coleman duP.: "A Progress Report on an Attempt to Construct an Invariant Model of Turbulent Shear Flows," A.R.A.P. Report No. 170, Oct. 1971.
3. Kolmogorov, A.N.: "Equations of Turbulent Motion of an Incompressible Fluid," Izv. Akad. Nauk, SSSR fiz. VI, No. 1-2, (1942), pp. 56-58.
4. Prandtl, L. and Wieghardt, K.: "Über ein neues Formelsystem für die ausgebildete Turbulenz," Nachr. Akad. Wiss. Goettingen 19, 6 (1945).
5. Chou, P.Y.: "Pressure Flow of a Turbulent Fluid between Two Infinite Parallel Planes," Quart. Appl. Math. 3, 3, (1949), pp. 198-209.
6. Rotta, J.: "Statistische Theorie nichthomogener Turbulenz," Z. Physik 129 (1951), p. 547.
7. Reynolds, Osborne: "On the Dynamical Theory of Incompressible Viscous Fluids and the Determination of the Criterion," Phil. Trans. Royal Society, London, A 186, (1894), p. 123.
8. Rosenbaum, Harold and Margolis, David P.: "Pressure Fluctuations beneath an Incompressible Turbulent Boundary Layer with Mass Addition," Physics of Fluids 10, 6 (1967), pp. 1231-1235.
9. Donaldson, Coleman duP., Sullivan, Roger D., and Rosenbaum, Harold: "A Theoretical Study of the Generation of Atmospheric Clear Air Turbulence," AIAA Journal 10, 2 (1972), pp. 162-170.
10. Cary, Aubrey M., Jr.: "Summary of Available Information on Reynolds Analogy for Zero-Pressure-Gradient, Compressible, Turbulent-Boundary-Layer Flow," NASA TN D-5560, 1970.

D

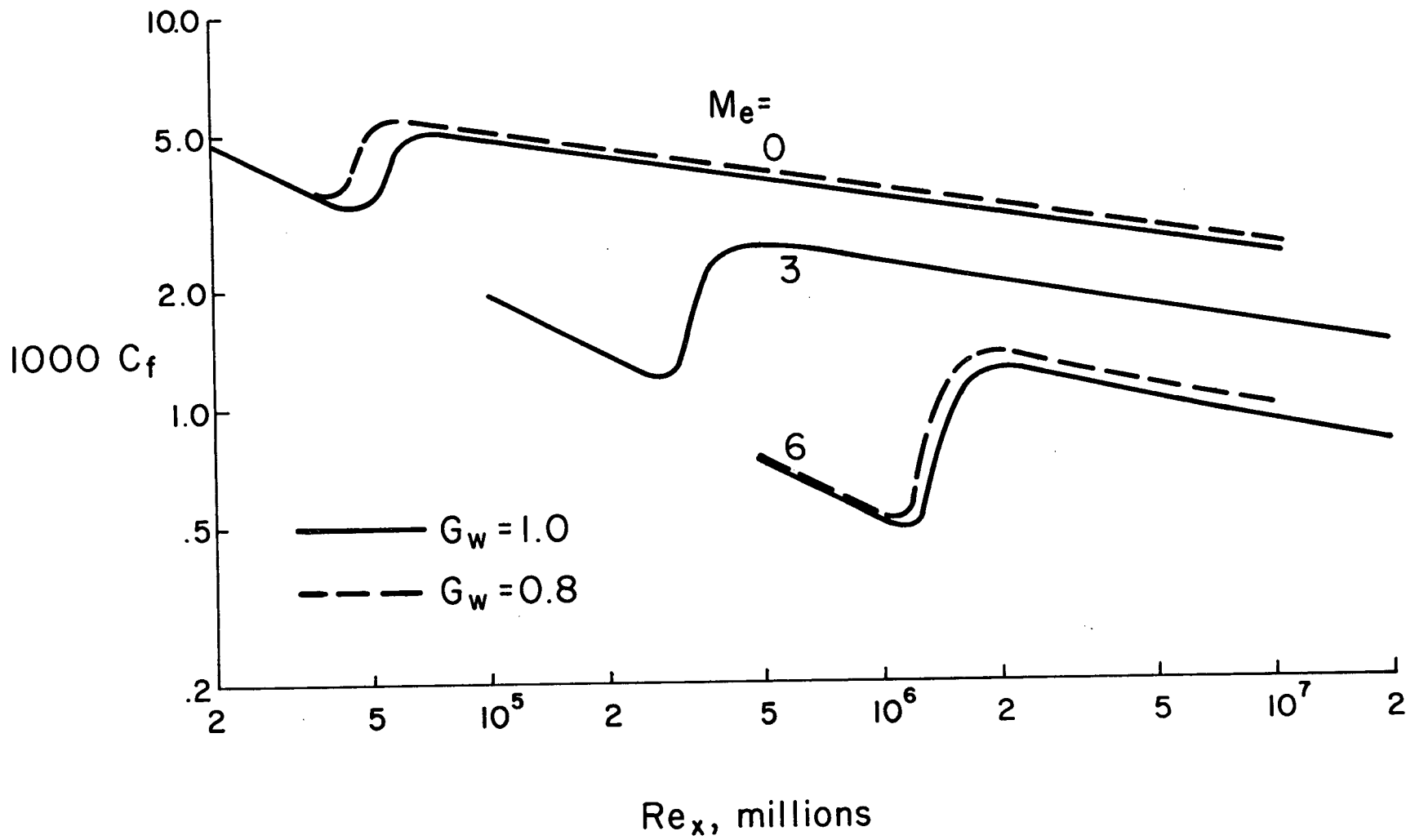


Figure 1. Skin-Friction Coefficient as a Function of Reynolds Number

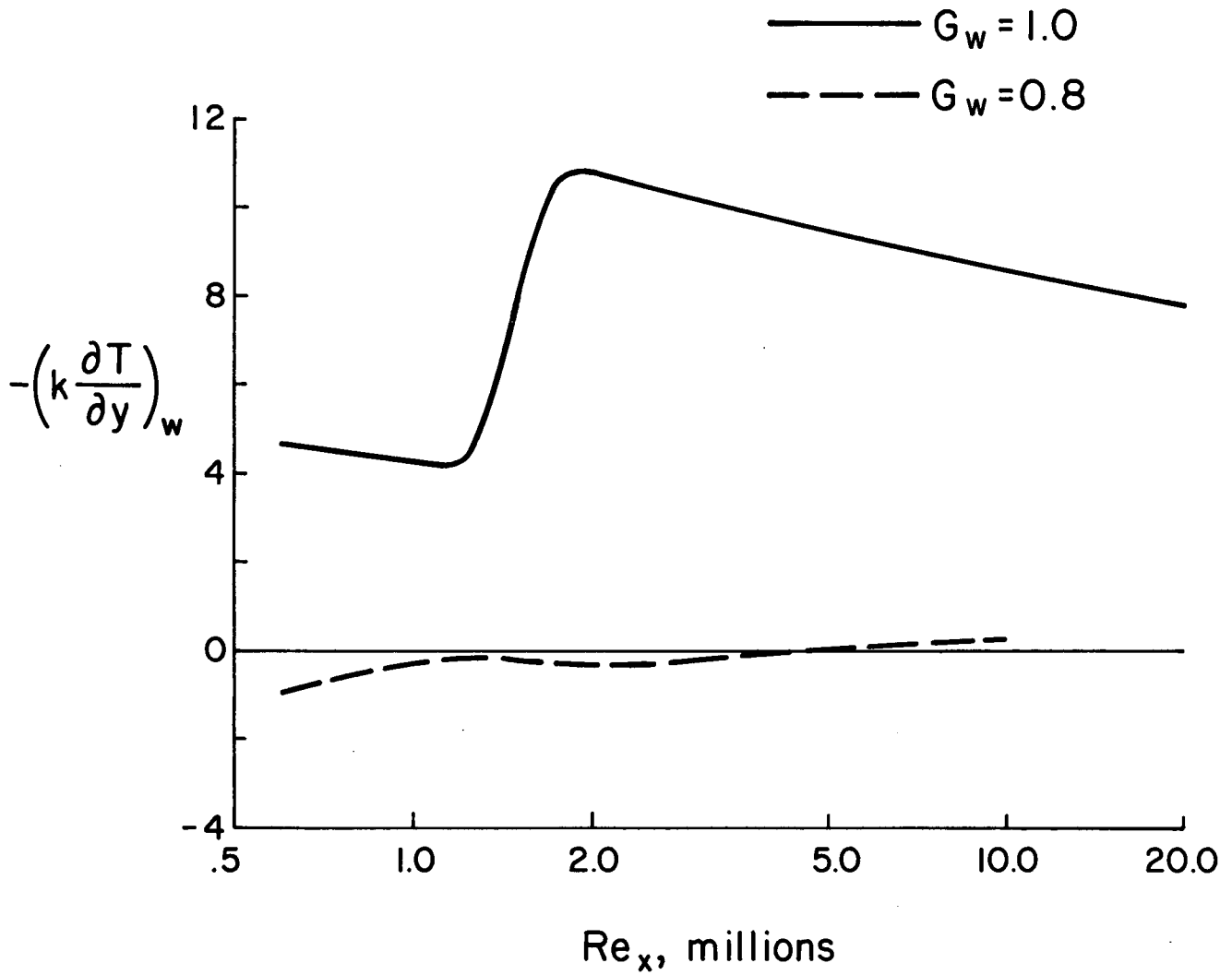


Figure 2. Heat Transfer at the Wall as a Function of Reynolds Number for $M_e = 6$

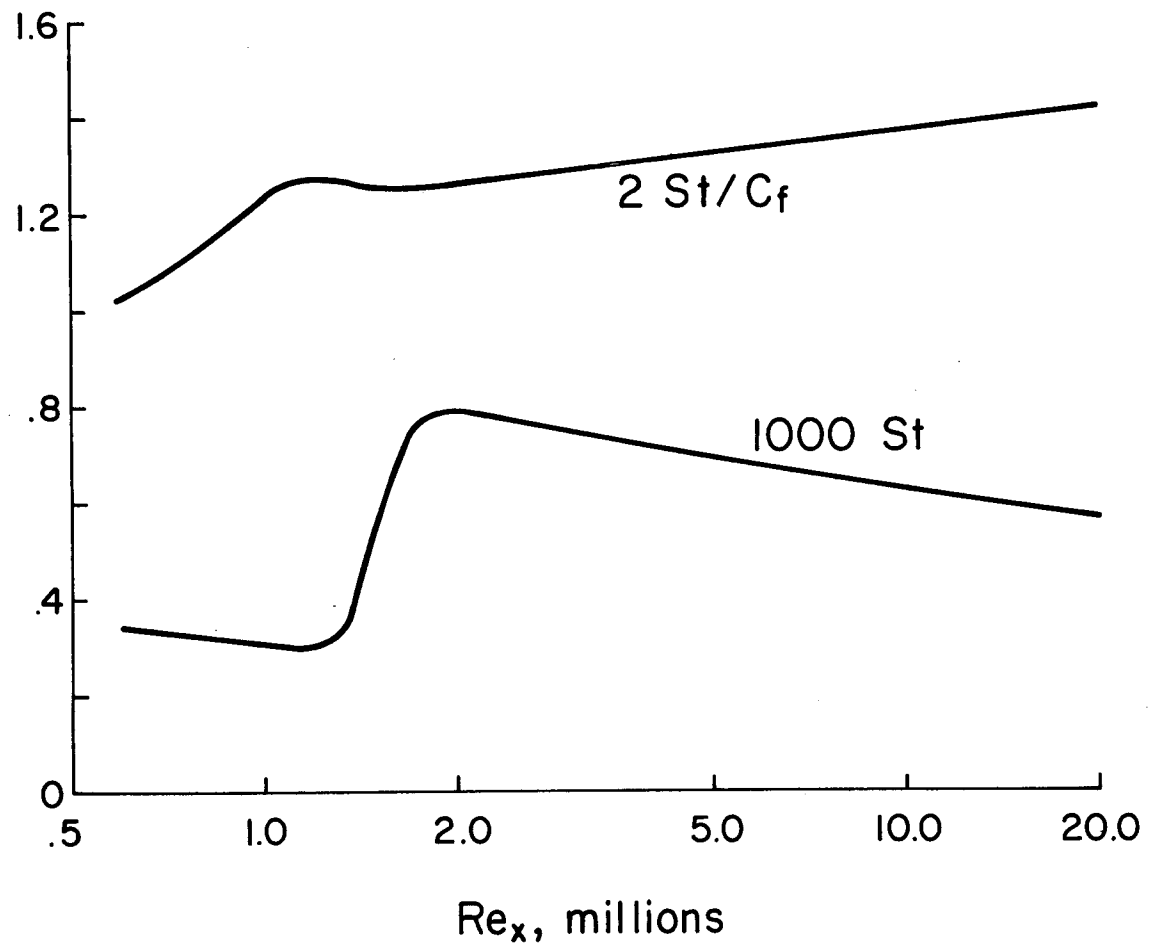


Figure 3. Stanton Number and Reynolds Analogy Factor as a Function of Reynolds Number for $M_e = 6$, $G_w = 1$

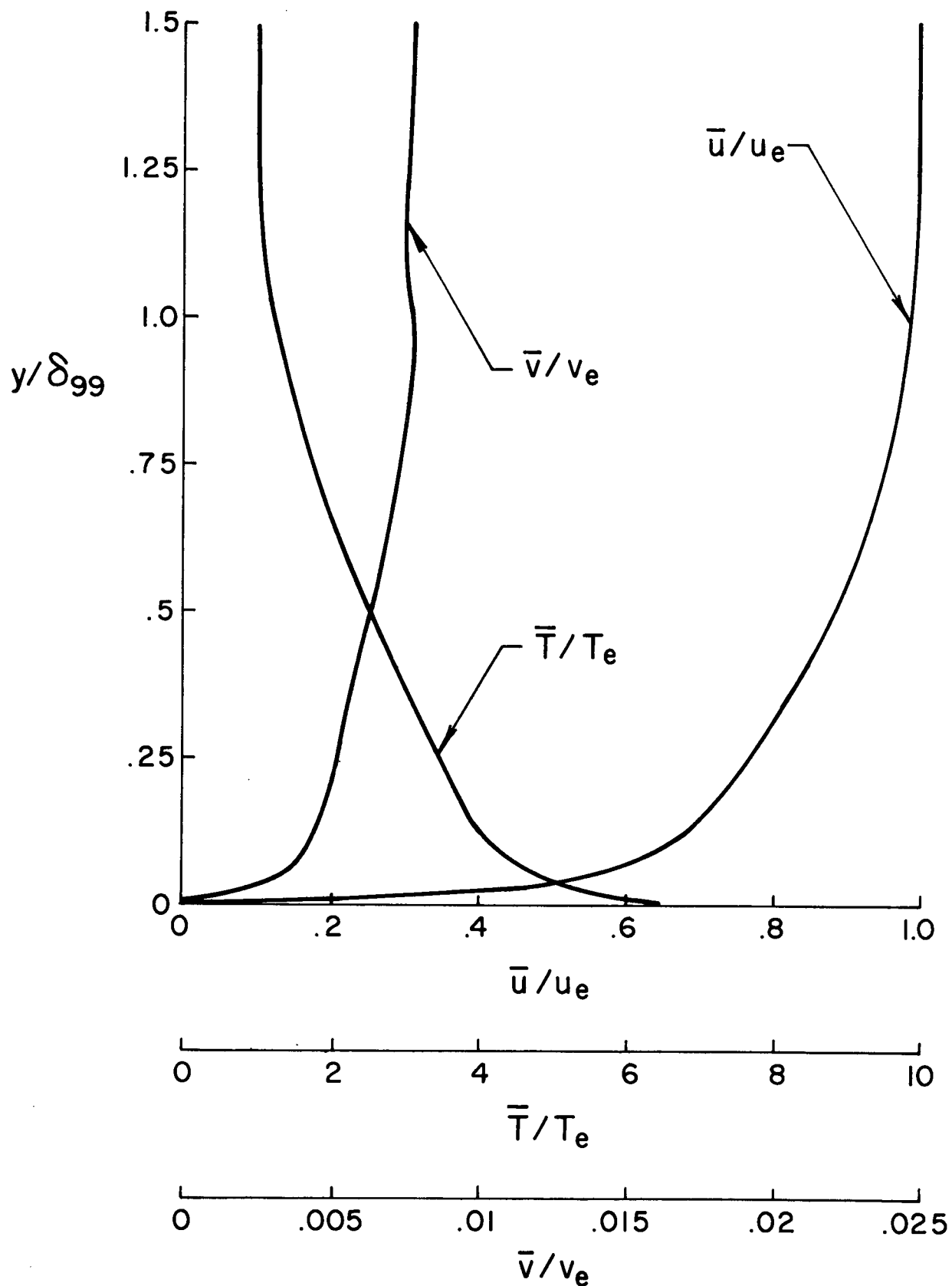


Figure 4. Profiles for $M_e = 6$, $G_w = 0.8$, $Re_x = 10$ Million

25

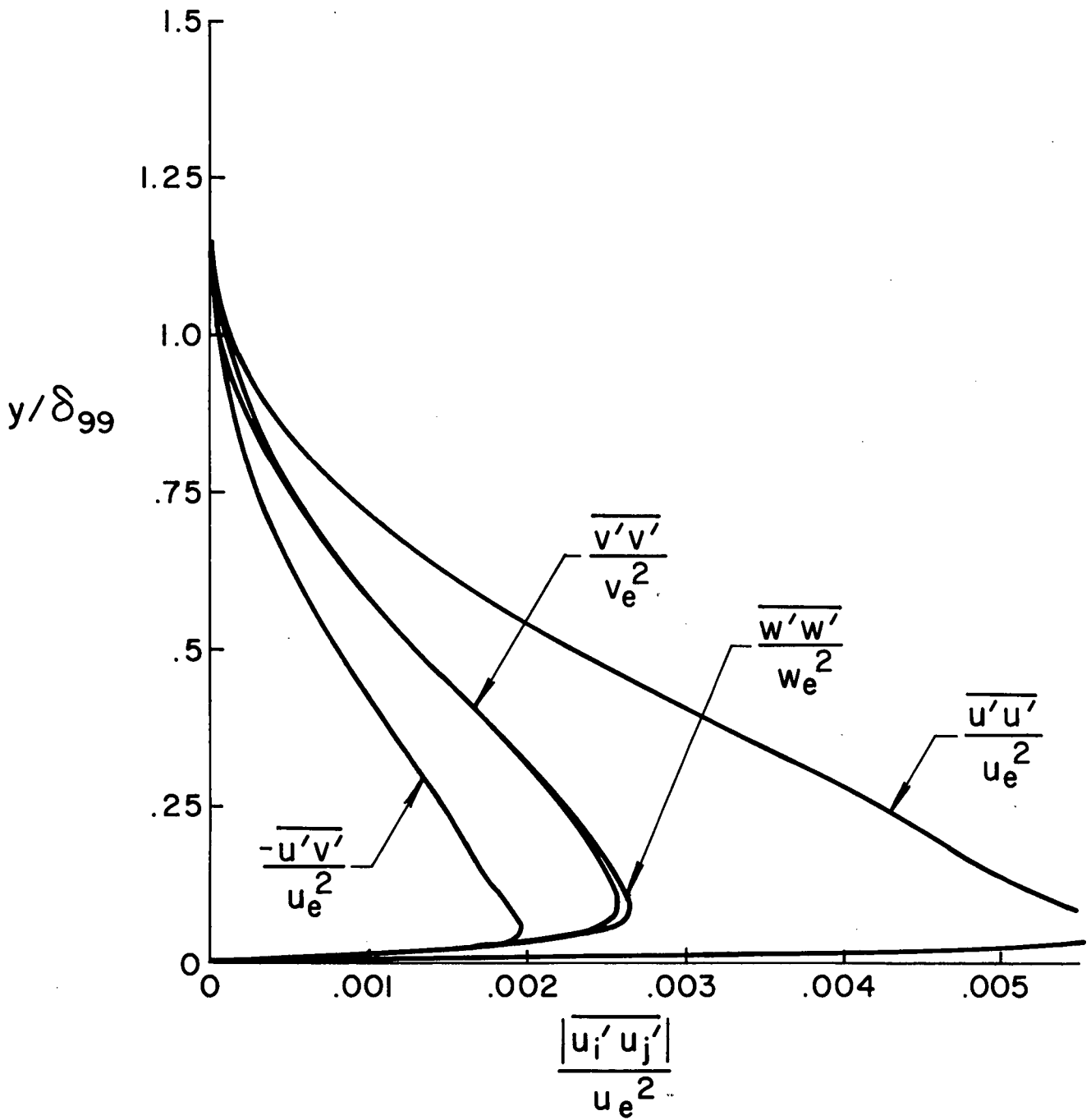


Figure 5. Profiles for $M_e = 6$, $G_w = 0.8$, $Re_x = 10$ Million

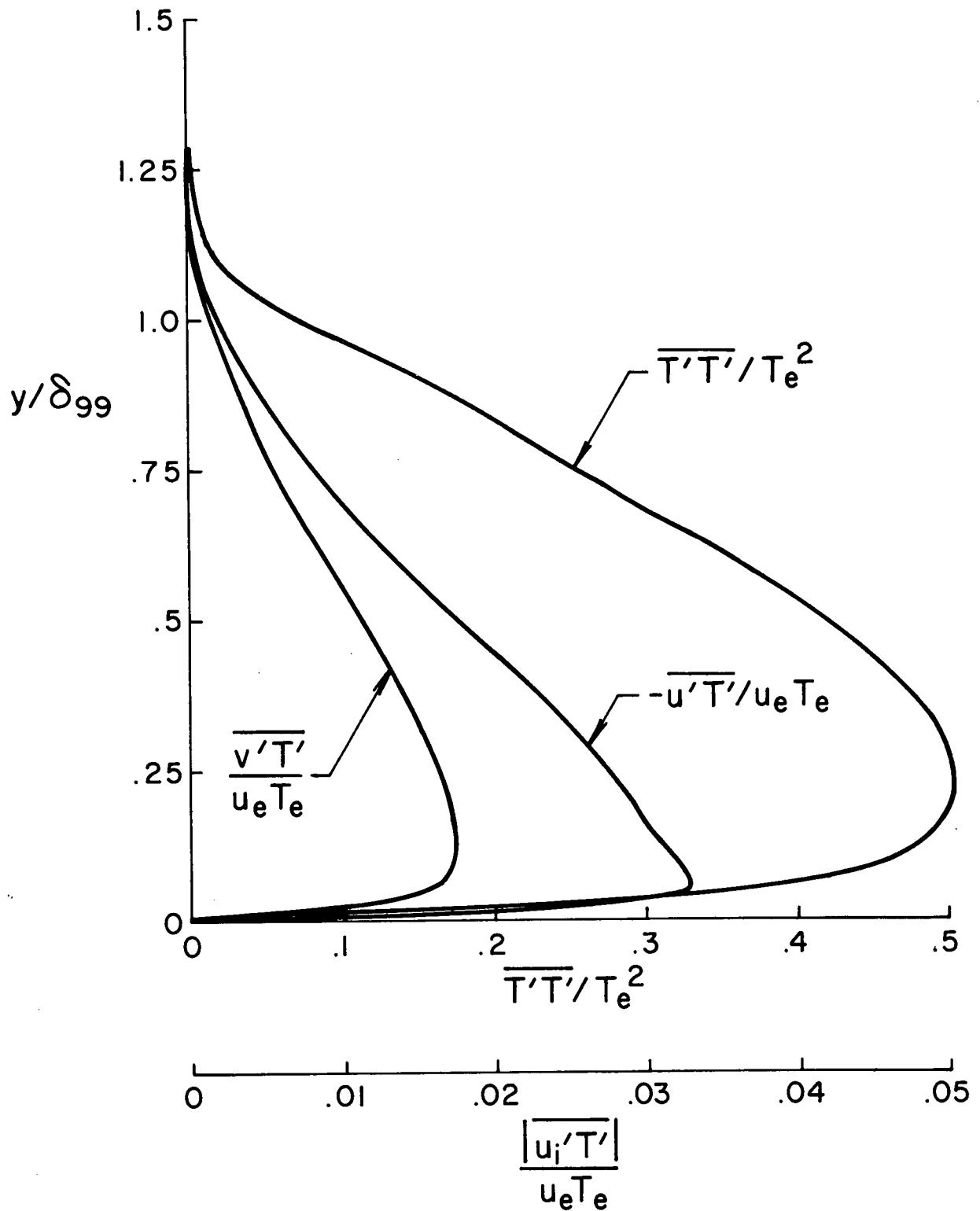


Figure 6. Profiles for $M_e = 6$, $G_w = 0.8$, $Re_x = 10$ Million

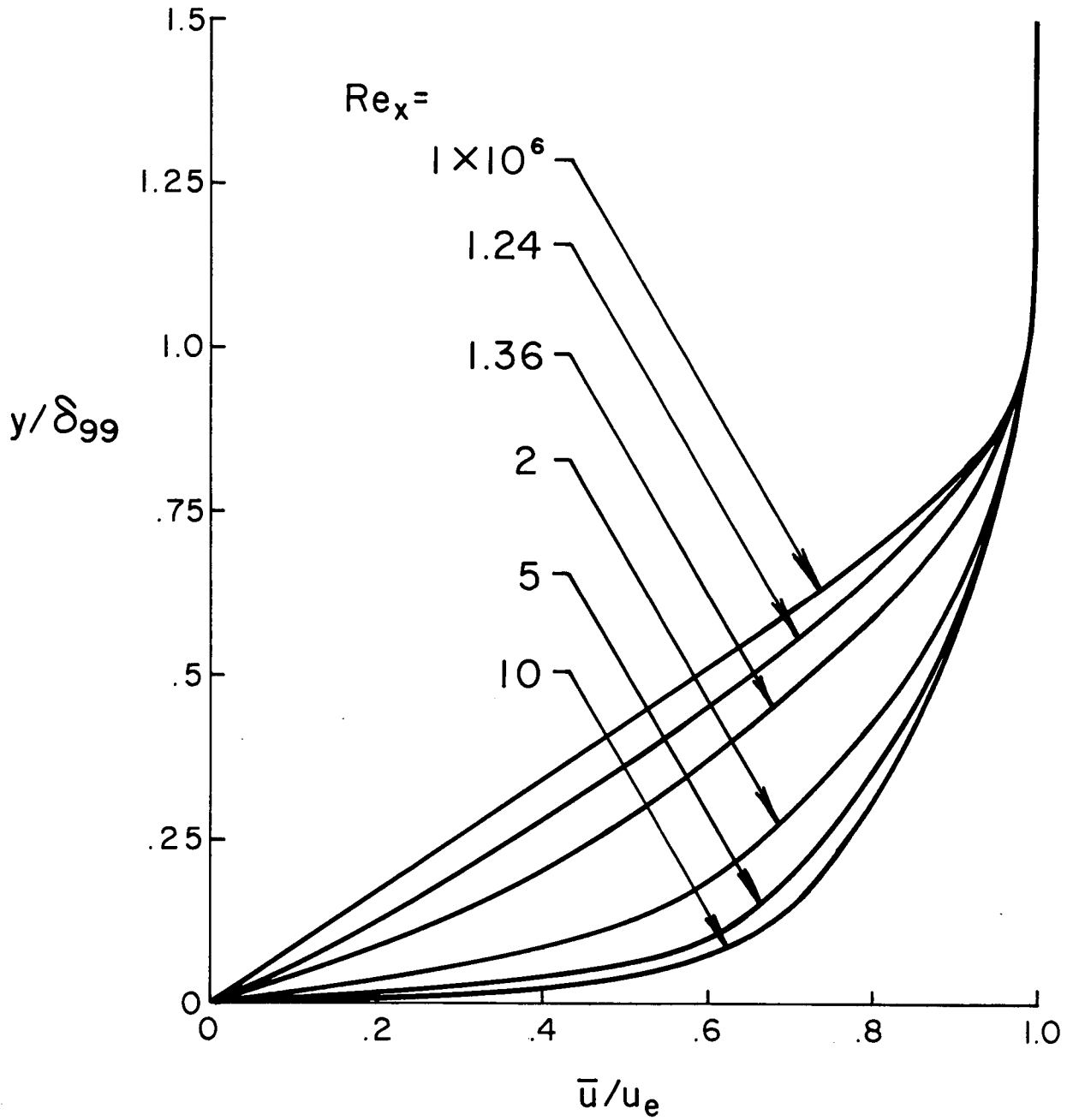


Figure 7. Profiles of \bar{u} for $M_e = 6$, $G_w = 0.8$

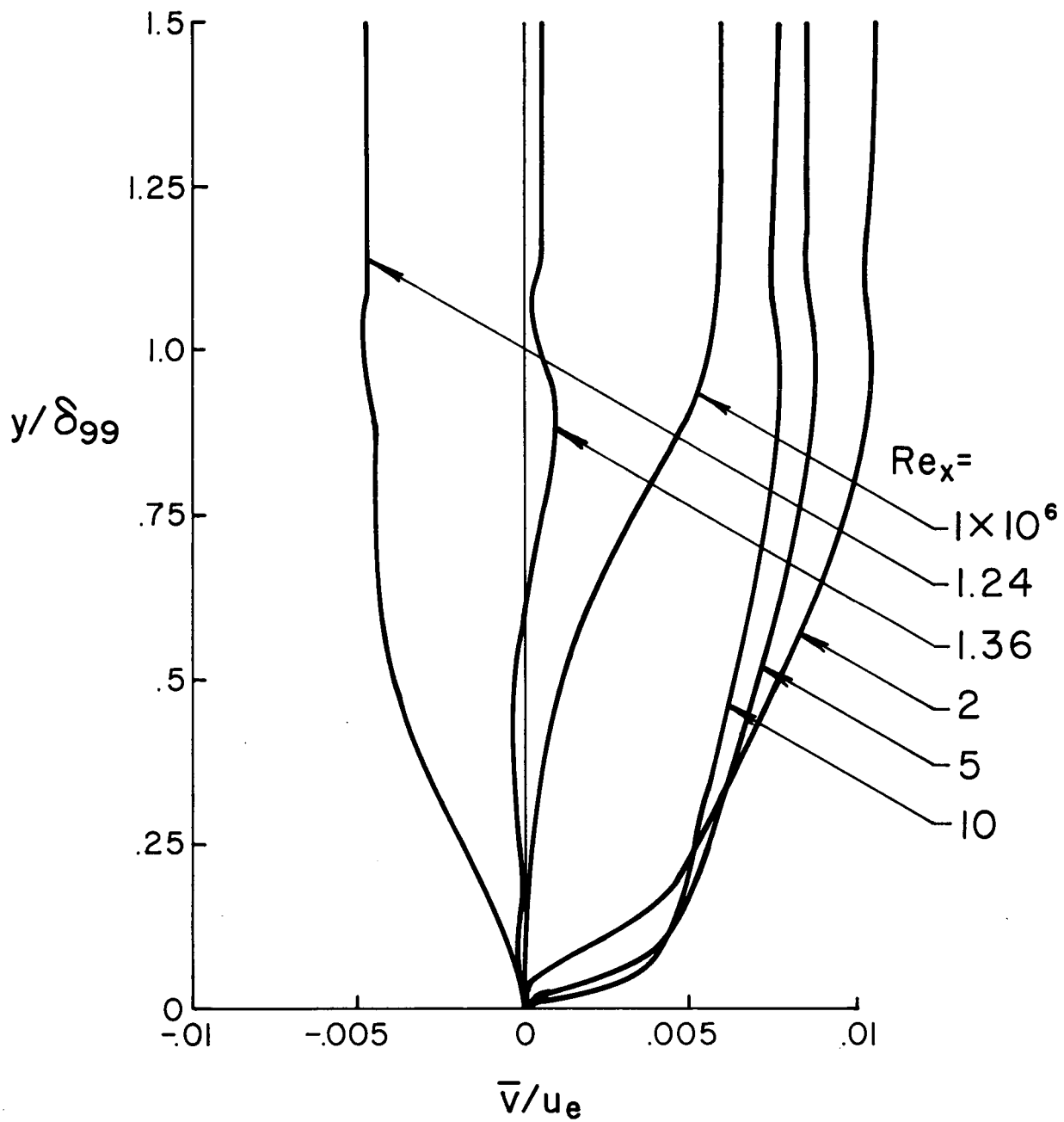


Figure 8. Profiles of \bar{v} for $M_e = 6$, $G_w = 0.8$

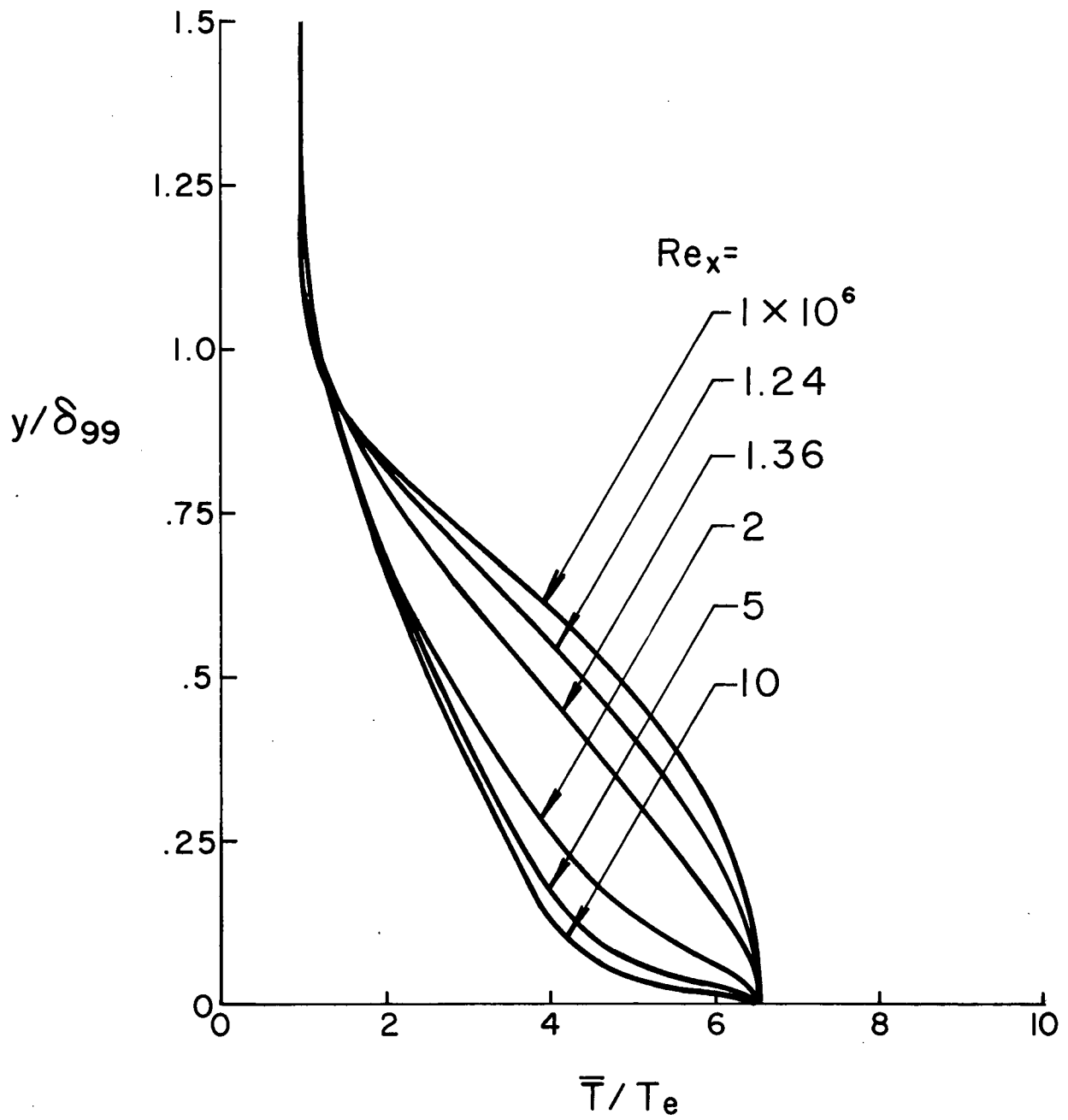


Figure 9. Profiles of \bar{T} for $M_e = 6$, $G_w = 0.8$

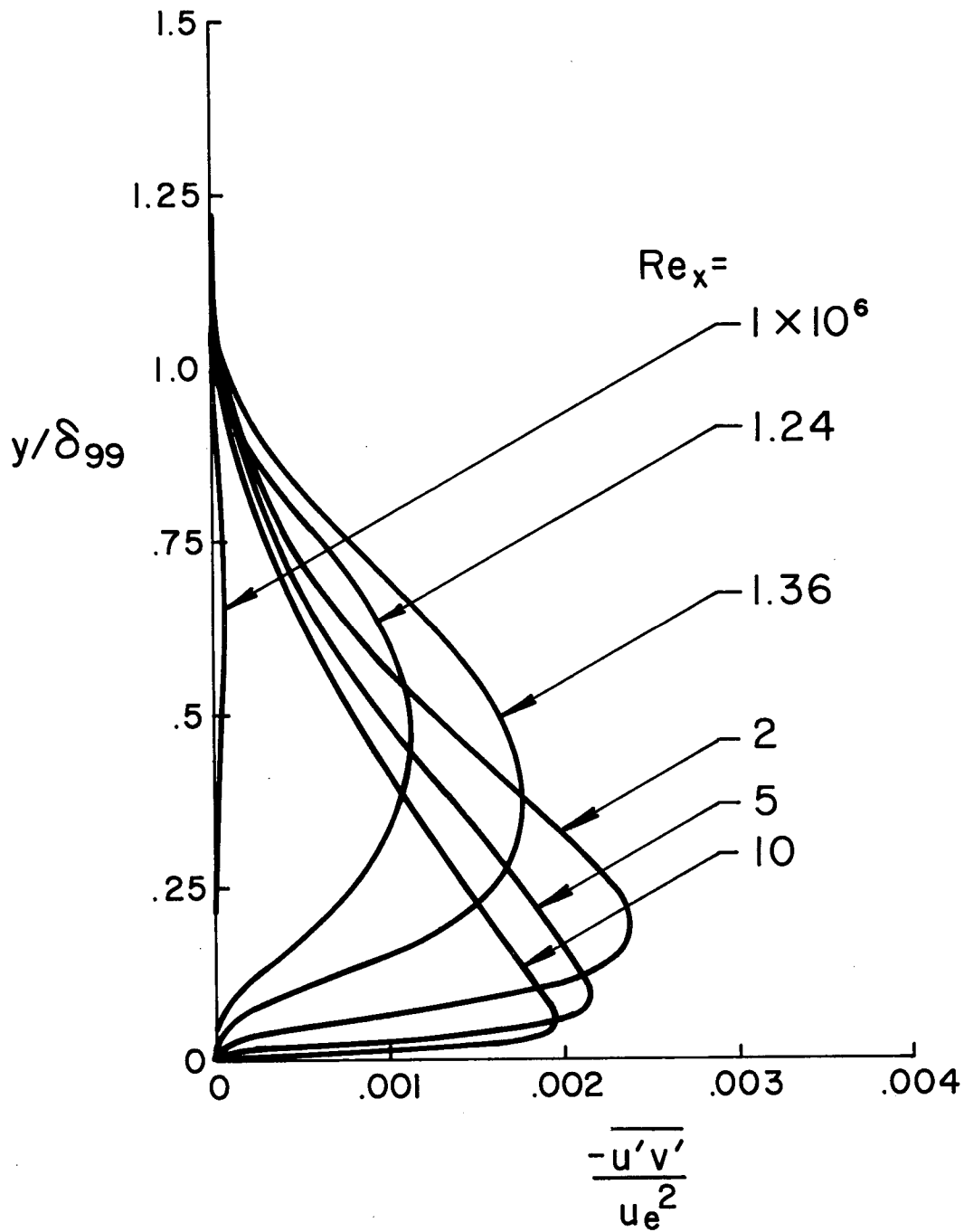


Figure 10. Profiles of $\overline{u'v'}$ for $M_e = 6$, $G_w = 0.8$

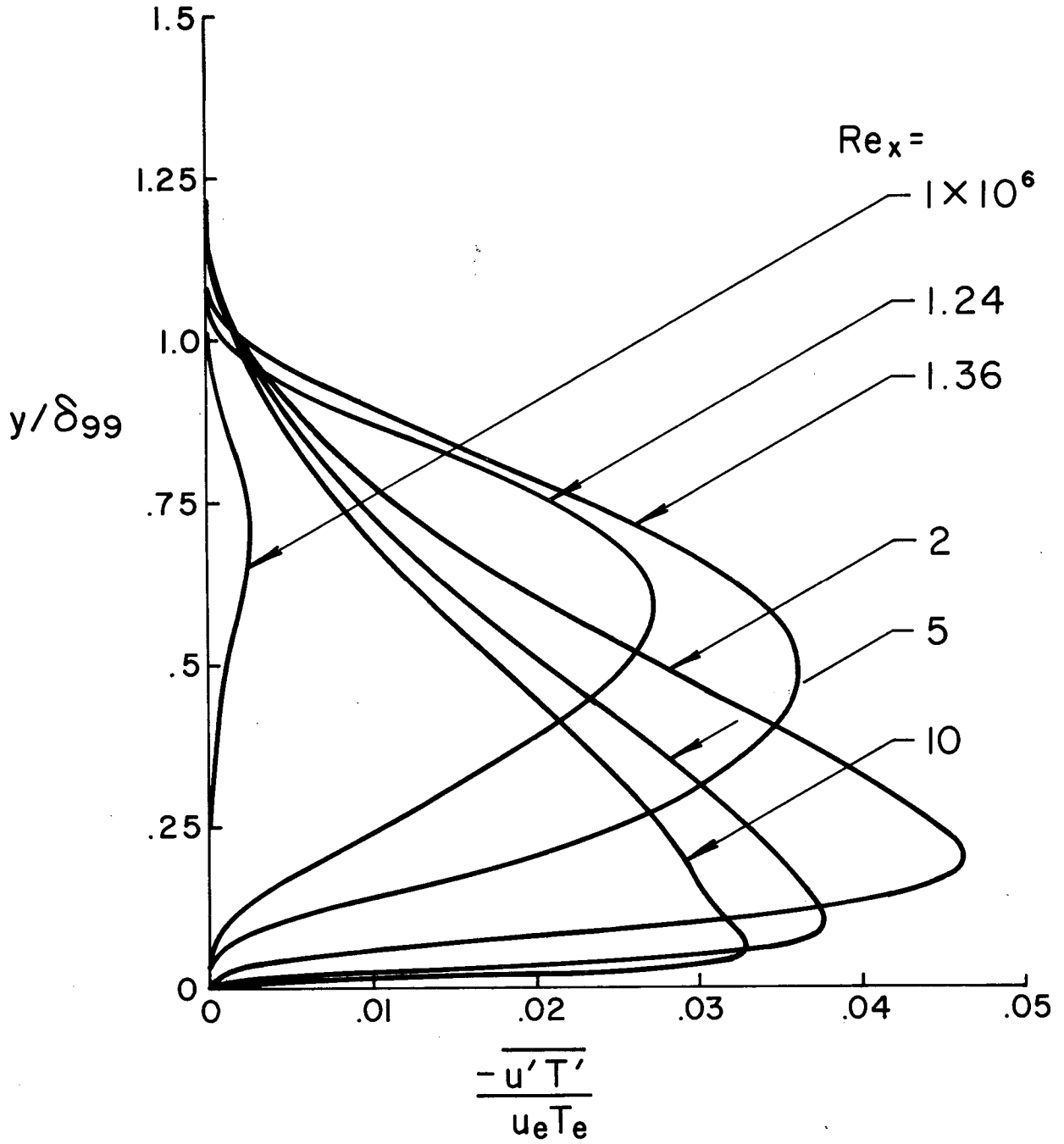


Figure 11. Profiles of $\overline{u'T'}$ for $M_e = 6$, $G_w = 0.8$

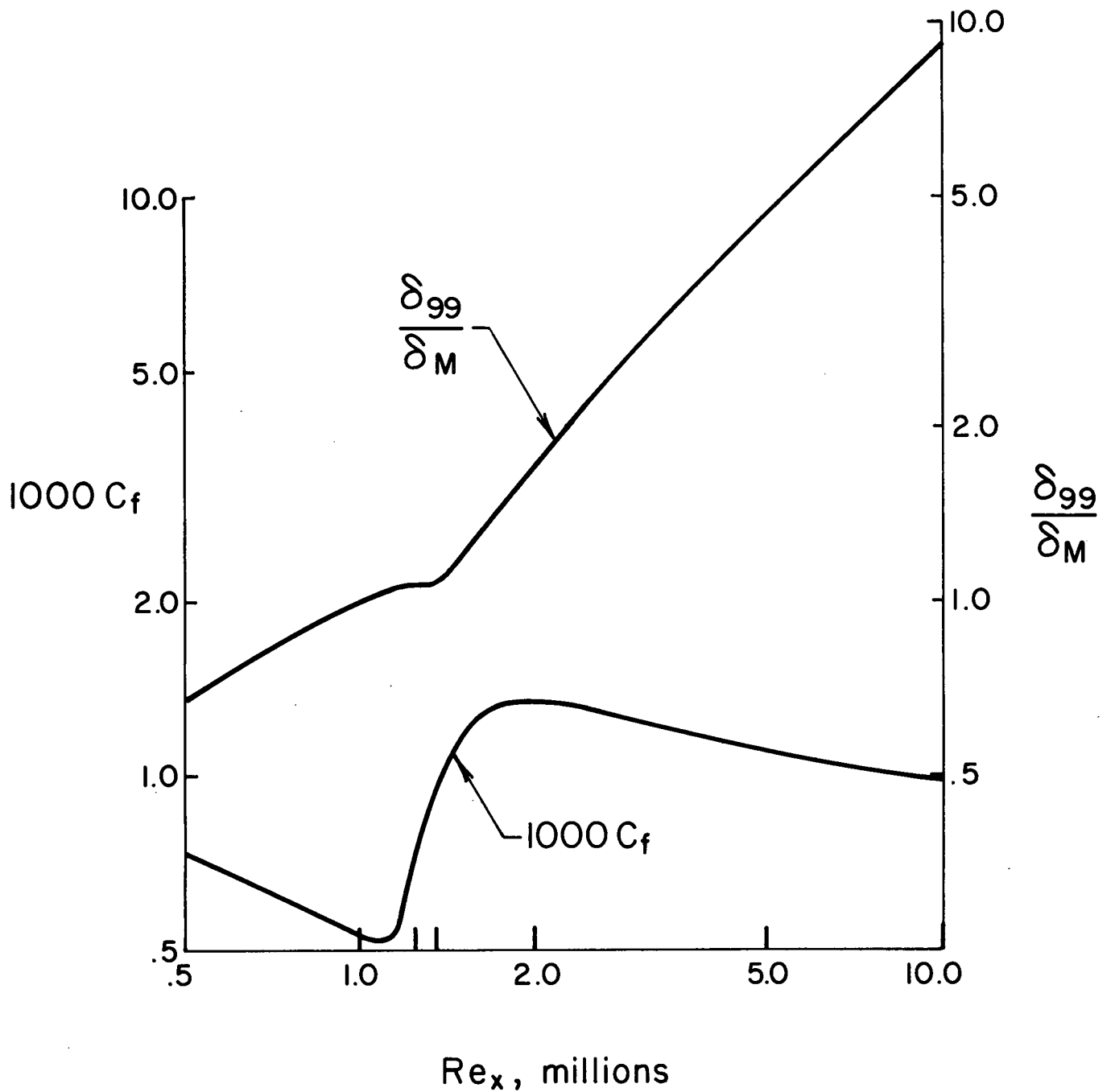


Figure 12. Coefficient of Friction and δ_{99} as a Function of Reynolds Number. δ_M is the value of δ_{99} for $Re_x = 10^6$. Vertical marks on the horizontal axis indicate the values of Re_x for which profiles are shown in Figs. 7-11 and Figs. 13-17.

ε

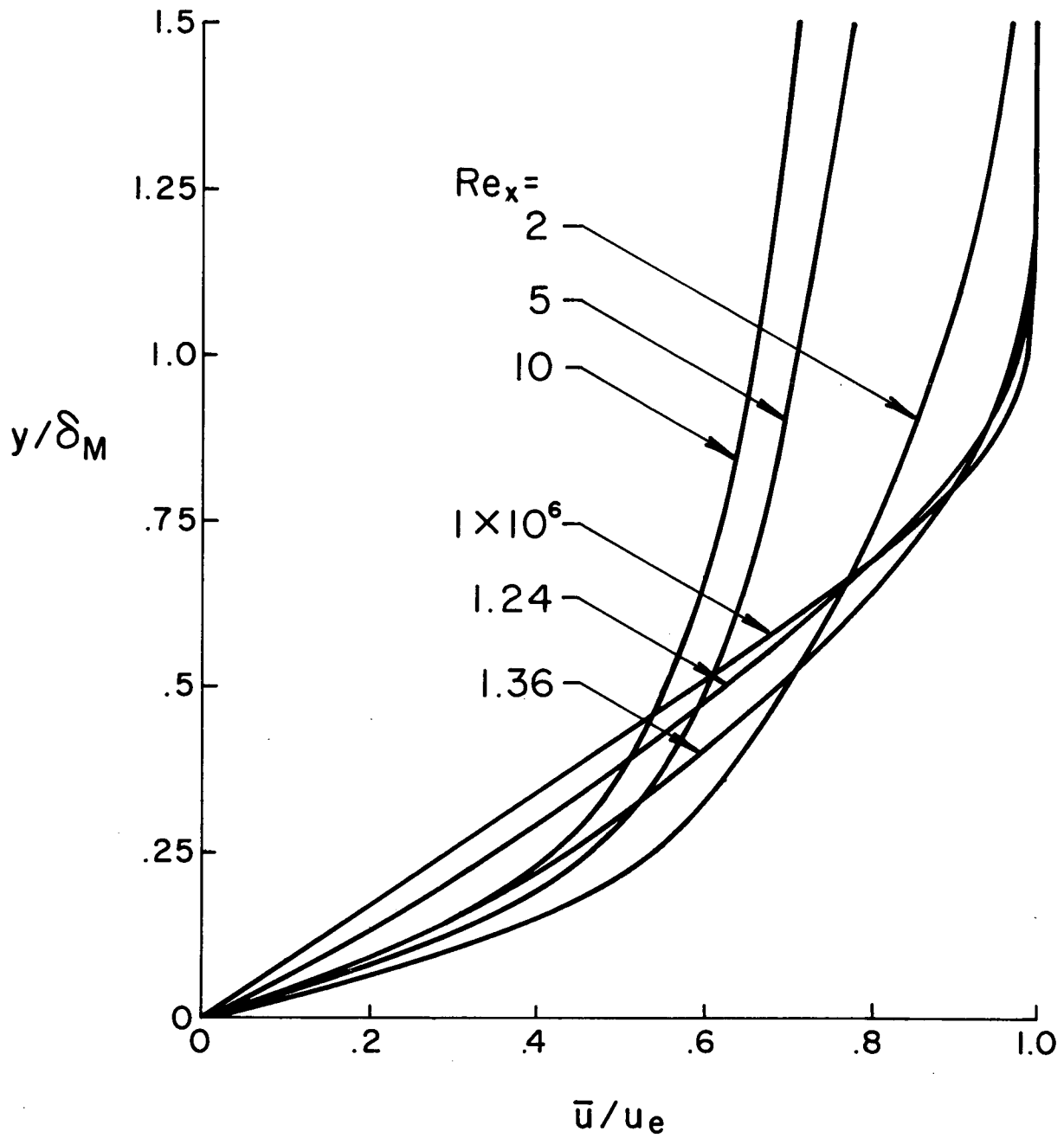


Figure 13. Profiles of \bar{u} for $M_e = 6$, $G_w = 0.8$.
 δ_M is the value of δ_{99} for $Re_x = 10^6$.

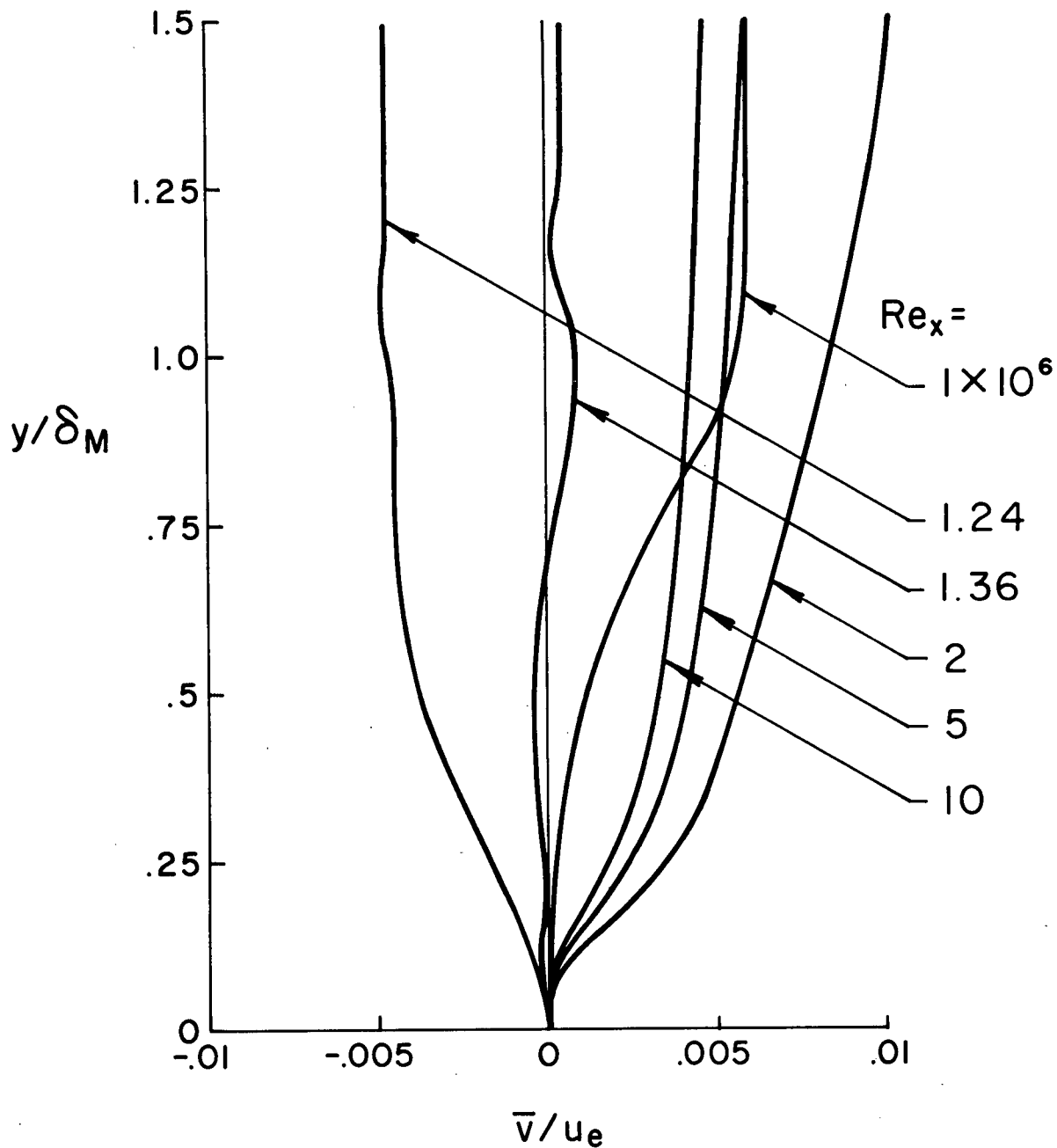


Figure 14. Profiles of \bar{v} for $M_e = 6, G_w = 0.8$.
 δ_M is the value of δ_{99} for
 $Re_x = 10^6$

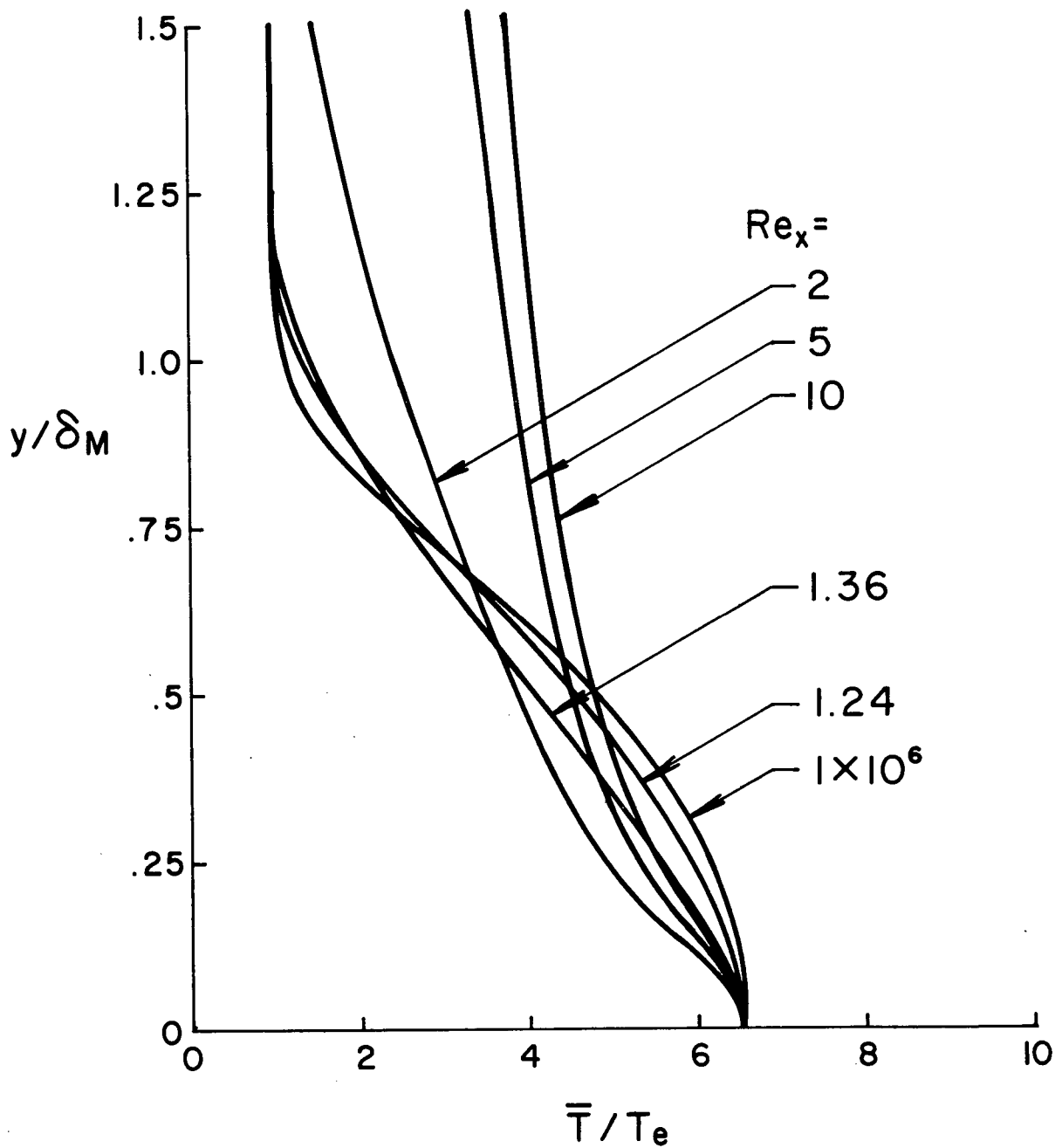


Figure 15. Profiles of \bar{T} for $M_e = 6$, $G_w = 0.8$.
 δ_M is the value of δ_{99} for
 $Re_x = 10^6$

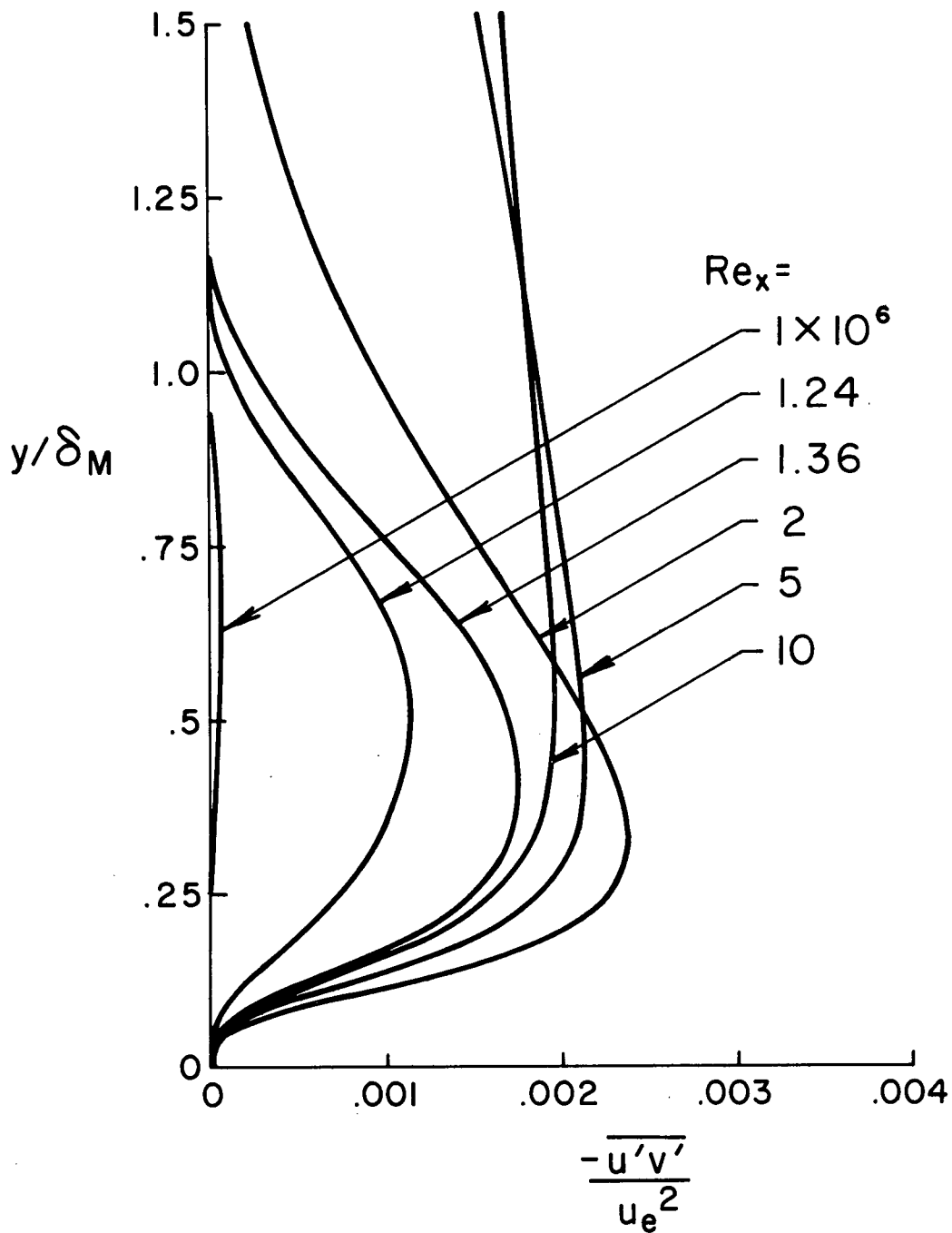


Figure 16. Profiles of $\overline{u'v'}$ for $M_e = 6$, $G_w = 0.8$.
 δ_M is the value of δ_{99} for $Re_x = 10^6$

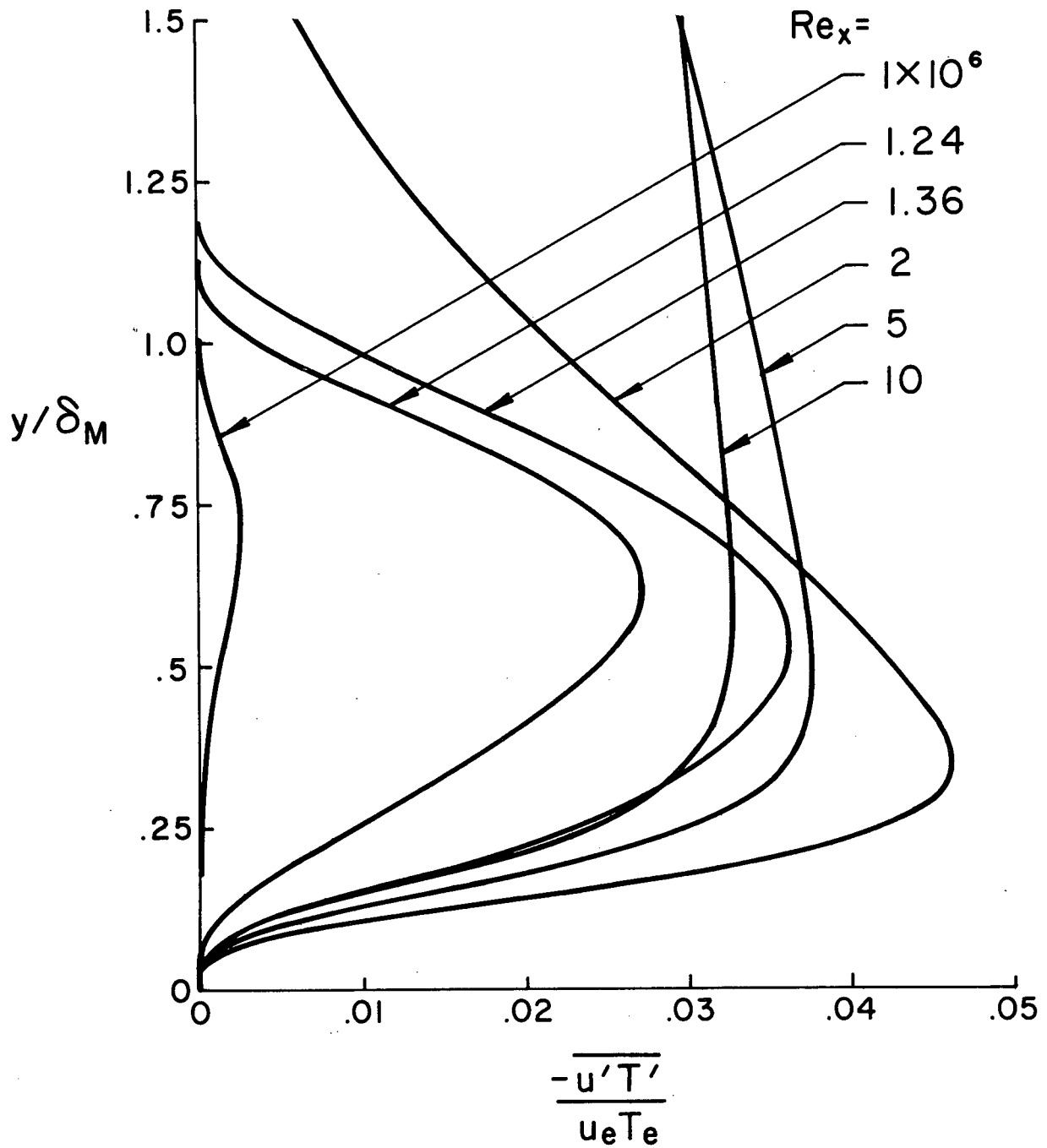


Figure 17. Profiles of $\overline{u'T'}$ for $M_e = 6$, $G_w = 0.8$.
 δ_M is the value of δ_{99} for
 $Re_x = 10^6$

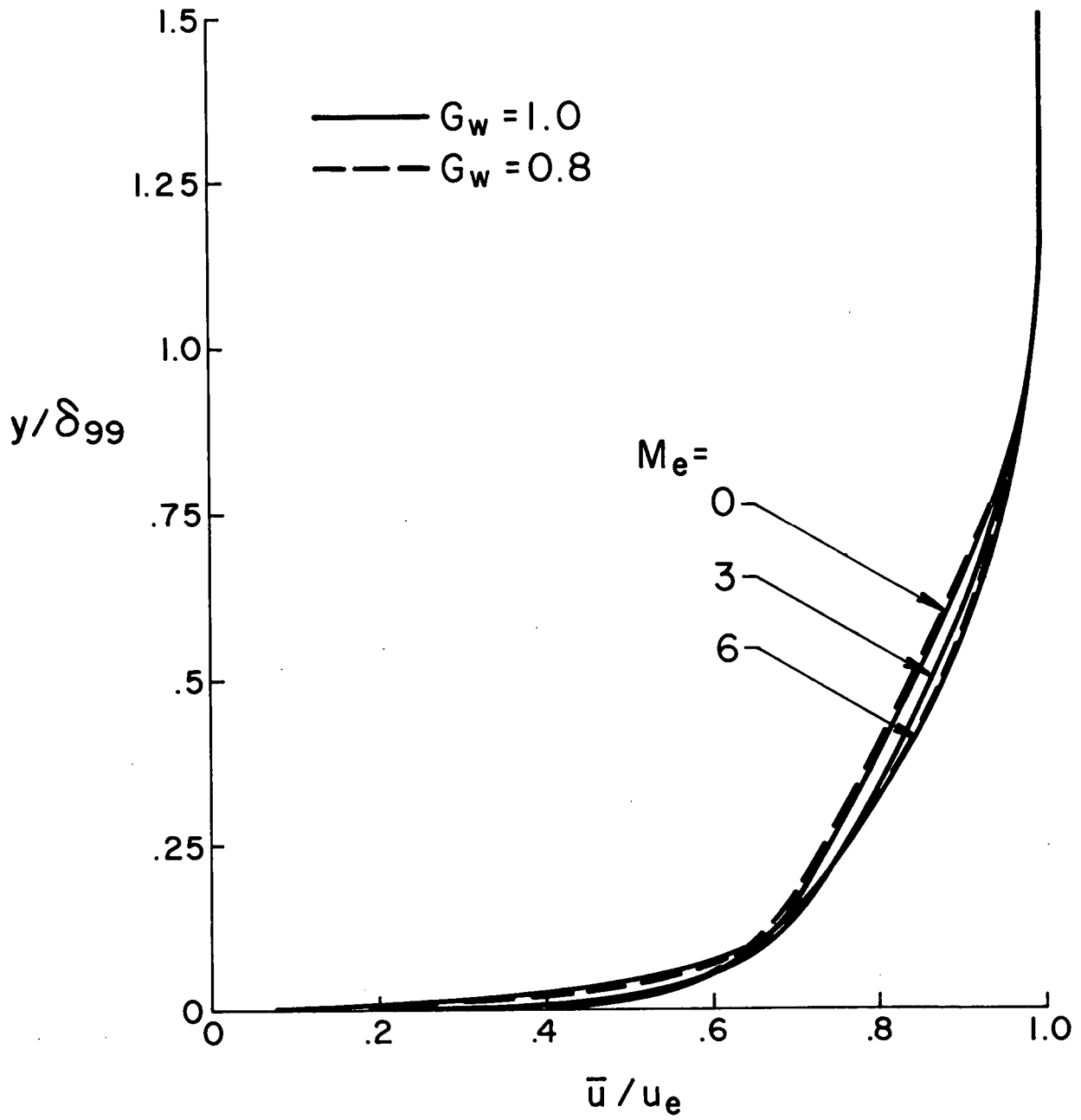


Figure 18. Profiles of \bar{u} for $Re_x = 10$ Million

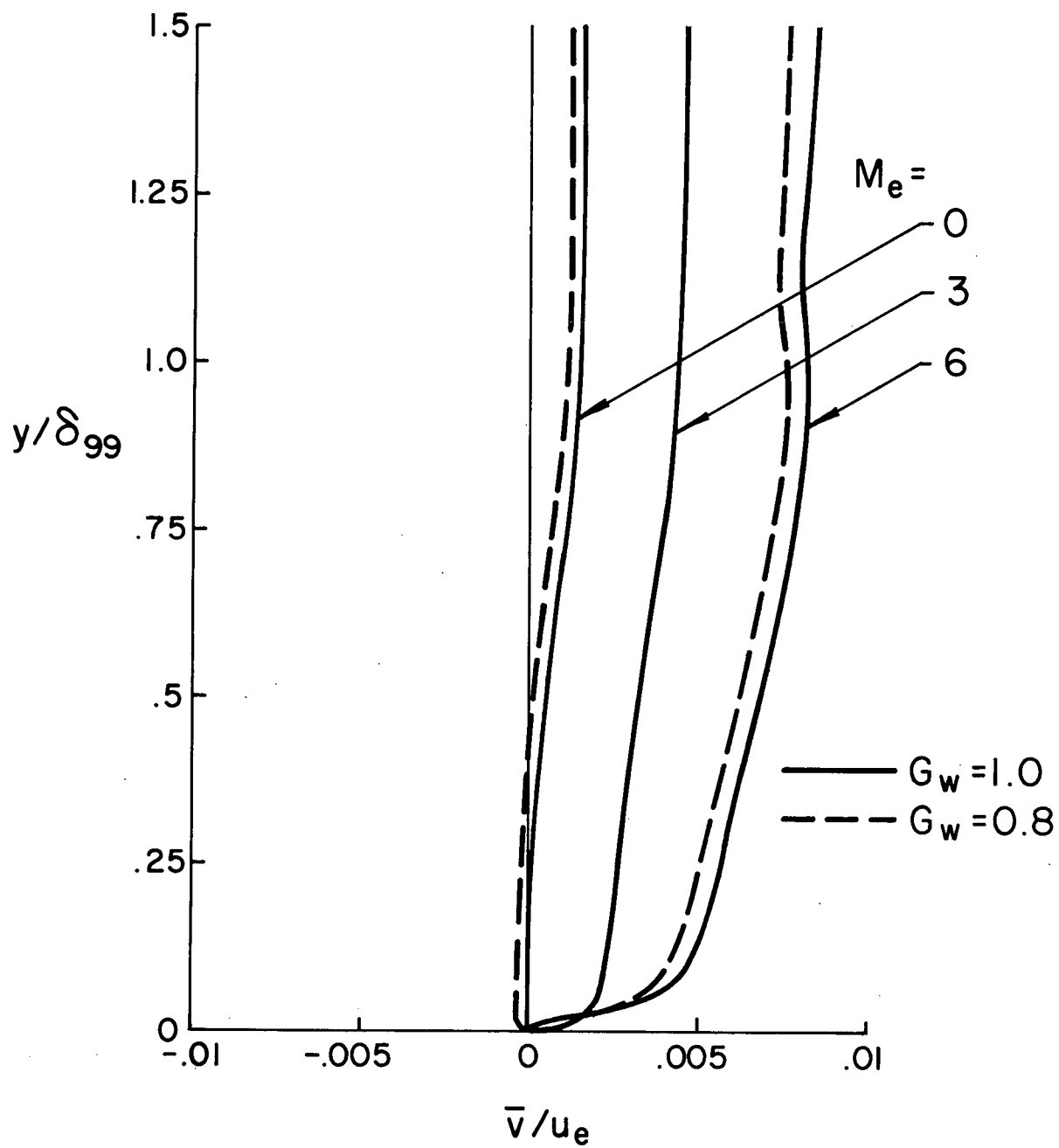


Figure 19. Profiles of \bar{v} for $Re_x = 10$ Million

40

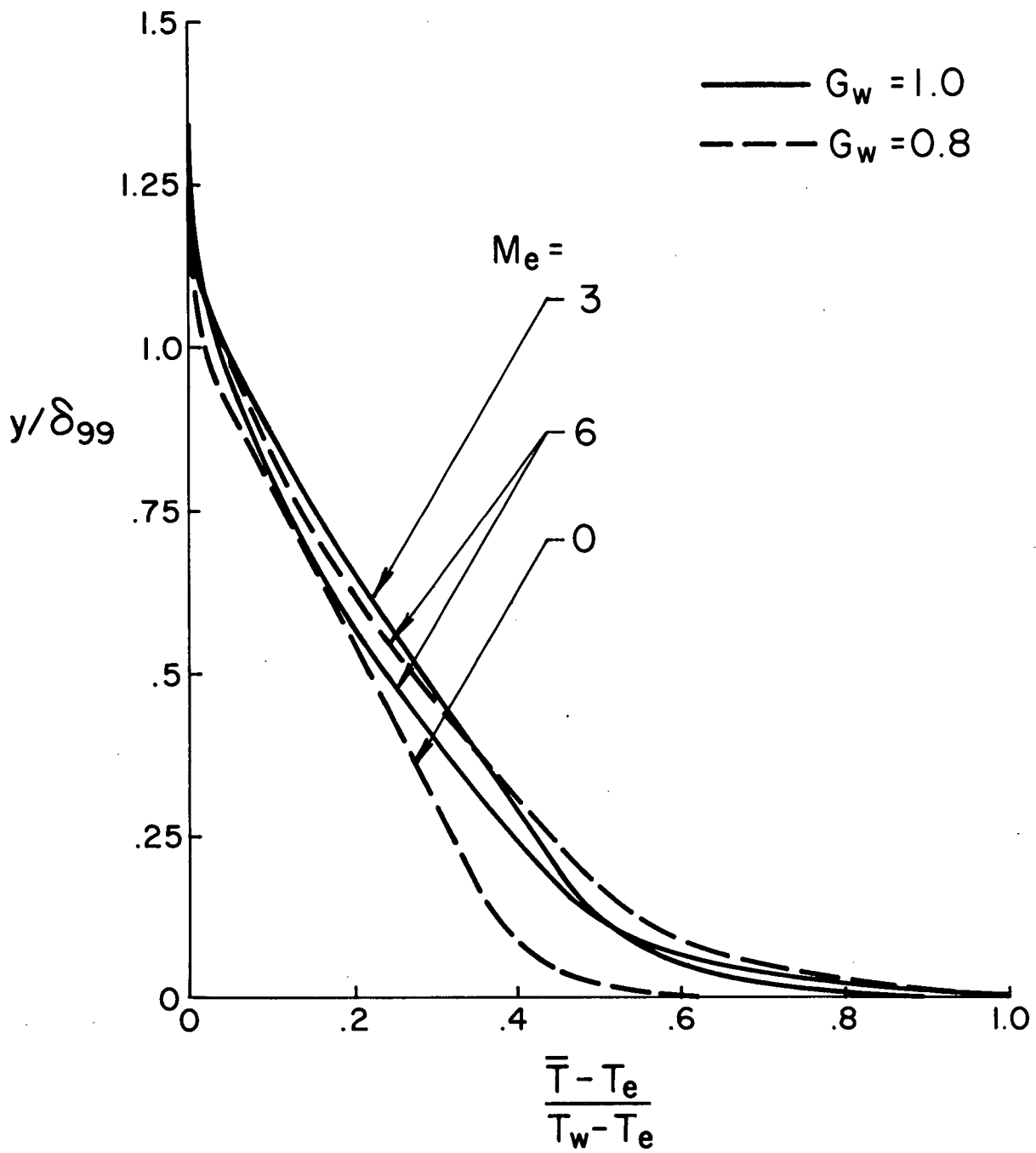


Figure 20. Profiles of \bar{T} for $Re_x = 10$ Million

HI

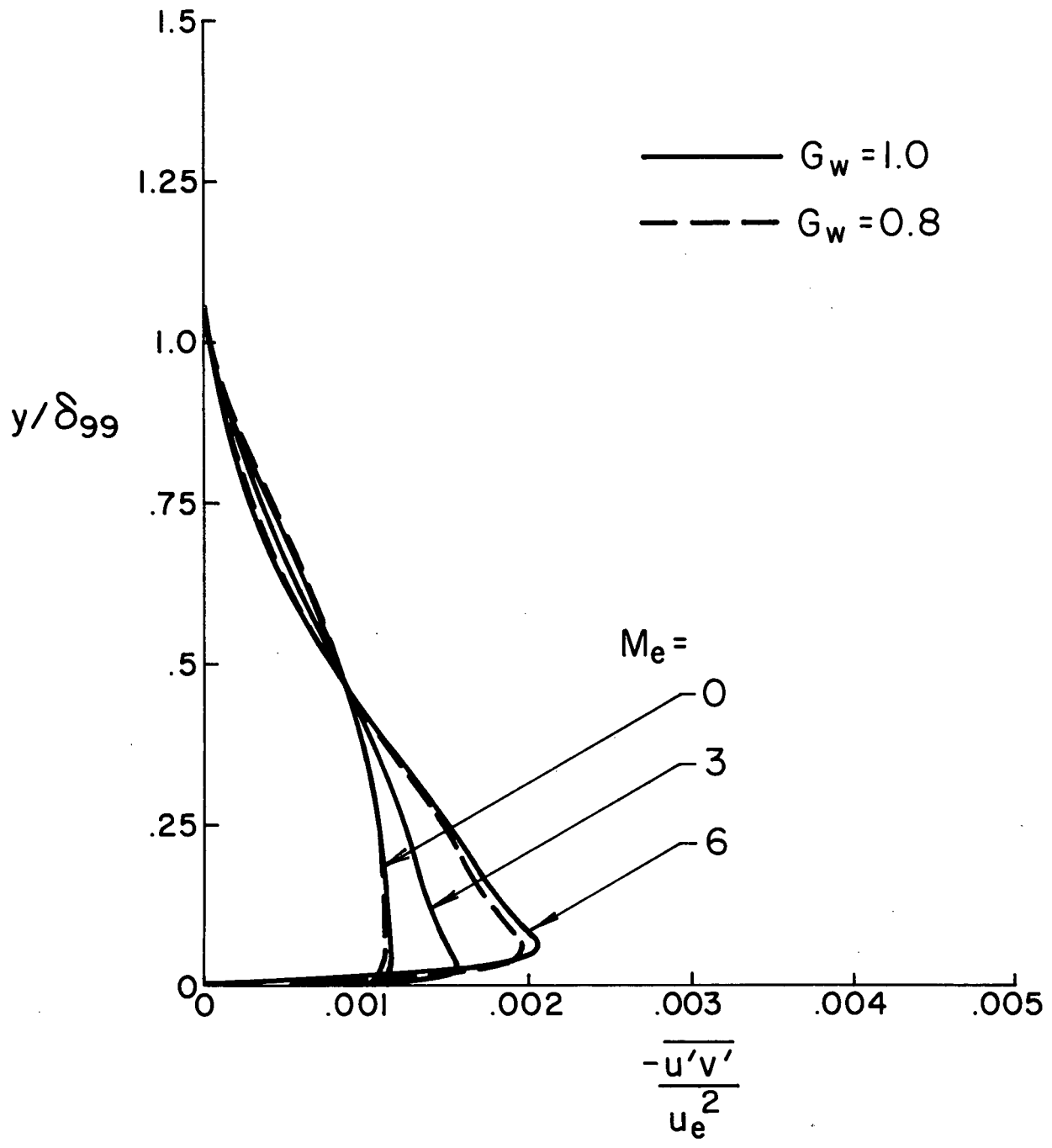


Figure 21. Profiles of $\overline{u'v'}$ for $Re_x = 10$ Million

42

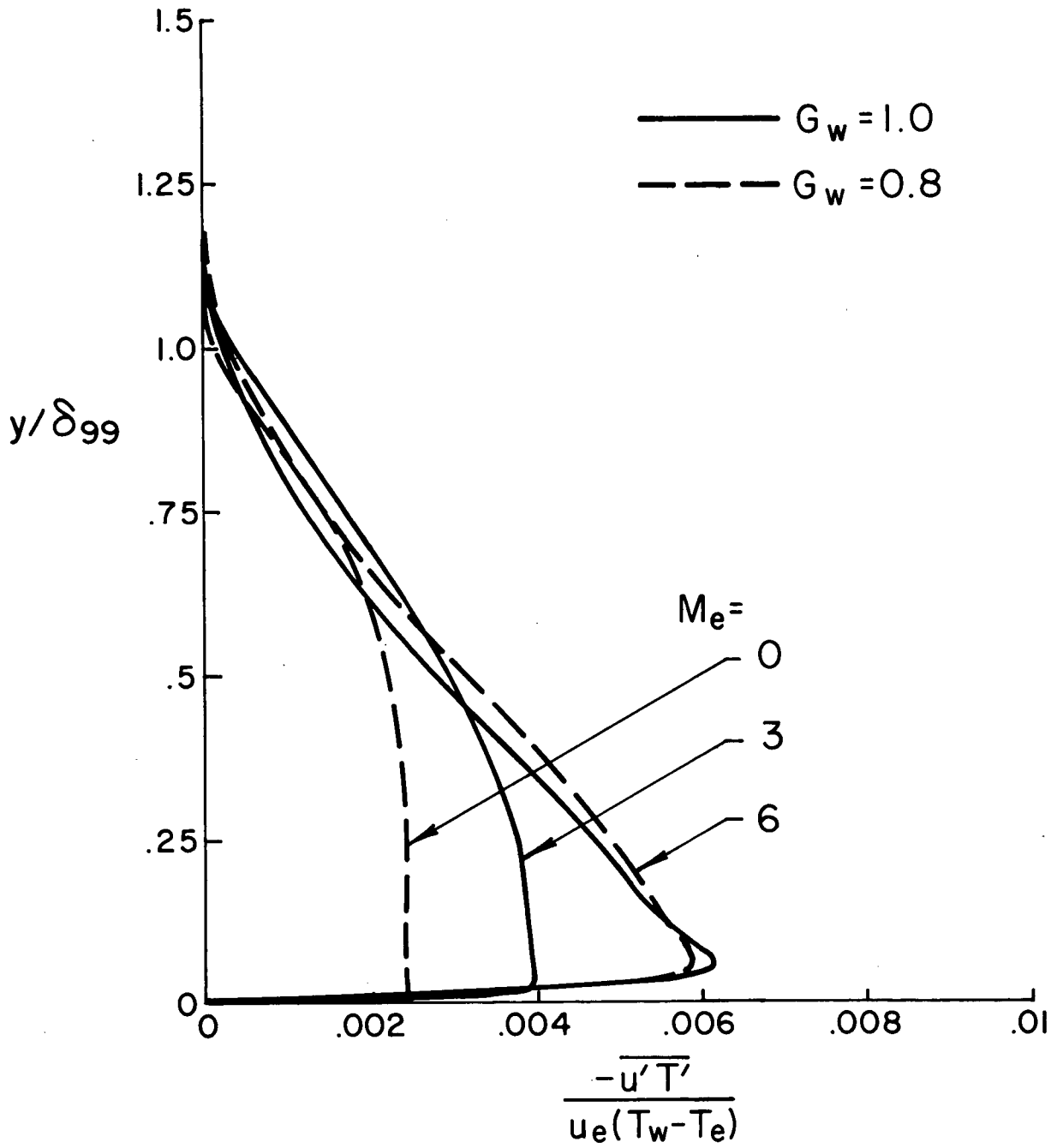


Figure 22. Profiles of $\overline{u'T'}$ for $Re_x = 10$ Million

43